Tetrachloro- and Tetrabromoarsonium(V) Cations: Raman and ^{75}As, ^{19}F NMR Spectroscopic Characterization and X-ray Crystal Structures of $[AsCl_4][As(OTeF_5)_6]$ and $[AsBr_4][AsF(OTeF_5)_5]$†

Michael Gerken,‡ Peter Kolb,‡ Andreas Wegner,‡ Hélène P. A. Mercier,‡ Horst Borrmann,§ David A. Dixon,|| and Gary J. Schrobilgen*,‡

Department of Chemistry, McMaster University, Hamilton, Ontario L8S 4M1, Canada, Max-Planck-Institut für Festkörperforschung, Heisenbergstrasse 1, Stuttgart D-70569, Germany, and William R. Wiley Environmental Molecular Sciences Laboratory, Pacific Northwest National Laboratory, 906 Batelle Boulevard, P.O. Box 999, KI-83, Richland, Washington 99352

Received February 4, 2000

The salts $[AsX_4][As(OTeF_5)_6]$ and $[AsBr_4][AsF(OTeF_5)_5]$ (X = Cl, Br) have been prepared by oxidation of AsX_3 with $XOTeF_5$ in the presence of the $OTeF_5$ acceptors $As(OTeF_5)_5$ and $AsF(OTeF_5)_4$. The mixed salts $[AsCl_4][Sb(OTeF_5)_{6-n}Cl_{n-2}]$ and $[AsCl_4][Sb(OTeF_5)_{6-n}Cl_n]$ ($n \geq 2$) have also been prepared. The $AsBr_4^+$ cation has been fully structurally characterized for the first time in SO_2ClF solution by ^{75}As NMR spectroscopy and in the solid state by a single-crystal X-ray diffraction study of $[AsBr_4][AsF(OTeF_5)_5]$: $P\bar{1}$, $a = 9.778(4)$ Å, $b = 17.731(7)$ Å, $c = 18.870(8)$ Å, $\alpha = 103.53(4)°$, $\beta = 103.53(4)°$, $\gamma = 105.10(4)°$, $V = 2915(2)$ Å^3, $Z = 4$, and $R_1 = 0.0368$ at −183 °C. The crystal structure determination and solution ^{75}As NMR study of the related $[AsCl_4][As(OTeF_5)_6]$ salt have also been carried out: $[AsCl_4][As(OTeF_5)_6]$, $R\bar{3}$, $a = 9.8741(14)$ Å, $c = 55.301(11)$ Å, $V = 4669(1)$ Å^3, $Z = 6$, and $R_1 = 0.0438$ at −123 °C; and $R\bar{3}$, $a = 19.688(3)$ Å, $c = 55.264(11)$ Å, $V = 18552(5)$ Å^3, $Z = 24$, and $R_1 = 0.1341$ at −183 °C. The crystal structure of the $As(OTeF_5)_6^-$ salt reveals weaker interactions between the anion and cation than in the previously known AsF_6^- salt. The $AsF(OTeF_5)_5^-$ anion is reported for the first time and is also weakly coordinating with respect to the $AsBr_4^+$ cation. Both cations are undistorted tetrahedra with bond lengths of 2.041(5)−2.056(3) Å for $AsCl_4^+$ and 2.225(2)−2.236(2) Å for $AsBr_4^+$. The Raman spectra are consistent with undistorted AsX_4^+ tetrahedra and have been assigned under T_d point symmetry. The $^{35}Cl/^{37}Cl$ isotope shifts have been observed and assigned for $AsCl_4^+$, and the geometrical parameters and vibrational frequencies of all known and presently unknown PnX_4^+ (Pn = P, As, Sb, Bi; X = F, Cl, Br, I) cations have been calculated using density functional theory methods.

Introduction

With the exception of bismuth, examples of tetrahalopnicogen(V) cations are known for all remaining group 15 elements. While only the fluoro-[1,2] and chlorocations[3] are known for nitrogen, all the tetraphosphonium(V) cations have been synthesized and are the most fully characterized series of tetrahalopnicogen cations, with crystal structure determinations for PCl_4^+,[4−8] PBr_4^+,[9,10] and PI_4^+,[11] ^{31}P NMR spectroscopic studies for PCl_4^+ and PBr_4^+,[12−16] and vibrational studies for PCl_4^+,[5,8,16−19] PBr_4^+,[16,18,20−22] and PI_4^+.[23] The PF_4^+ cation has only been characterized in the solid state by Raman spectroscopy.[24,25] Several $SbCl_4^+$ salts have been characterized by X-ray crystallography[26−28] and vibrational spectroscopy.[26,29] We recently reported a full characterization in solution by $^{121,123}Sb$

† Dedicated to the memory of Paul William Oberman (August 11, 1915 to February 19, 2000), dedicated mentor, colleague, and friend.

* To whom correspondence should be addressed.
‡ McMaster University.
§ Max-Planck-Institut.
|| Pacific Northwest National Laboratory.

(1) Christe, K. O. *Spectrochim. Acta* **1980**, *36A*, 921.
(2) Christe, K. O.; Lindt, M. D.; Thorup, N.; Russell, D. R.; Fawcett, J.; Bau, R. *Inorg. Chem.* **1988**, *27*, 2450.
(3) Minkwitz, R.; Bernstein, D.; Sawodny, W. *Angew. Chem., Int. Ed. Engl.* **1990**, *29*, 181.
(4) Preiss, H. *Z. Anorg. Allg. Chem.* **1971**, *380*, 56.
(5) Shamir, J.; Luski, S.; Cohen, S.; Gibson, D. *Inorg. Chem.* **1985**, *24*, 2301.
(6) Erdbrügger, C. F.; Jones, P. G.; Schelbach, R.; Schwarzmann, E.; Sheldrick, G. M. *Acta Crystallogr.* **1987**, *C43*, 1857.
(7) Preut, H.; Lennhoff, D.; Minkwitz, R. *Acta Crystallogr.* **1992**, *C48*, 1648.
(8) Gates, P. N.; Knachel, H. C.; Finch, A.; Fratini, A. V.; Fitch, A. N.; Nardone, O.; Otto, J. C.; Snider, D. A. *J. Chem. Soc., Chem. Commun.* **1995**, 2719.
(9) Gerding, H.; Nobel, P. C. *Recueil* **1958**, *77*, 472.
(10) Gabes, W.; Olie, K. *Acta Crystallogr.* **1970**, *26*, 443.
(11) Pohl, S. *Z. Anorg. Allg. Chem.* **1983**, *498*, 15.
(12) Wieker, W.; Grimmer, A *Z. Naturforsch.* **1966**, *21B*, 1103.
(13) Wieker, W.; Grimmer, A *Z. Naturforsch.* **1967**, *22B*, 257.
(14) Dillon, K. B.; Gates, P. N. *J. Chem. Soc., Chem. Commun.* **1972**, 348.
(15) Dillon, K. B.; Waddington, T. C.; Younger, D. *Inorg. Nucl. Chem. Lett.* **1973**, *9*, 63.
(16) Dillon, K. B.; Harris, R. K.; Gates, P. N.; Muir, A. S.; Root, A. *Spectrochim. Acta* **1991**, *47A*, 831.
(17) Reich, P.; Preiss, H. *Z. Chem.* **1967**, *7*, 115.
(18) Rafaeloff, R.; Shamir, J. *Spectrochim. Acta* **1974**, *30A*, 1305.
(19) Shamir, J.; van der Veken, B. J.; Herman, M. A.; Rafaeloff, R. *J. Raman Spectrosc.* **1981**, *11*, 215.
(20) Gabes, W.; Gerding, H. *Recueil* **1971**, *90*, 157.
(21) Gabes, W.; Olie, K.; Gerding, H. *Recueil* **1972**, *91*, 1367.
(22) Shamir, J.; Schneider, S.; van der Veken, B. J. *J. Raman Spectrosc.* **1986**, *17*, 463.
(23) Tornieporth-Oetting, I.; Klapötke, T. *J. Chem. Soc., Chem. Commun.* **1990**, 132.
(24) Chen, G. S. H.; Passmore, J. *J. Chem. Soc., Chem. Commun.* **1973**, 559.
(25) Chen, G. S. H.; Passmore, J. *J. Chem. Soc., Dalton Trans.* **1979**, 1251.
(26) Preiss, H. *Z. Anorg. Allg. Chem.* **1972**, *389*, 254.

10.1021/ic000118g CCC: $19.00
Published on Web 06/01/2000

NMR spectroscopy and in the solid state of the previously unknown $SbBr_4^+$ and known $SbCl_4^+$ cations as their $Sb(OTeF_5)_6^-$ salts.[30] The SbF_4^+ and SbI_4^+ cations are presently unknown.

All members of the AsX_4^+ (X = F, Cl, Br, I) series have been synthesized[31−35] and characterized by Raman spectroscopy,[36−44] and AsF_4^+ [44] and $AsCl_4^+$ [36] have also been characterized by infrared spectroscopy. The salts of AsF_4^+ and $AsCl_4^+$, namely, $[AsF_4][PtF_6]$,[44] $[AsCl_4][SbCl_6]\cdot AsCl_3$,[45] $[AsCl_4][AsF_6]$,[36,46,47] $[AsCl_4][AlCl_4]$, and $[AsCl_4][GaCl_4]$[35,40] are stable compounds, but only $[AsCl_4][SbCl_6]\cdot AsCl_3$[45] and $[AsCl_4][AsF_6]$[46,47] have been structurally characterized by single-crystal X-ray diffraction. Unstable $[AsBr_4][AsF_6]$ is formed by the reaction of Br_2, $AsBr_3$, and AsF_5 at −196 to −5 °C but begins to disproportionate at temperatures above −78 °C, leading to the formation of $AsBr_3$, Br_2, and AsF_3.[41,43] It has been proposed that the decomposition is initiated by fluoride ion transfer from the anion to the cation (eq 1), presumably by means of a fluorine bridge interaction between $AsBr_4^+$ and AsF_6^-, followed by successive redox eliminations of Br_2 (eqs 2 and 3) and disproportionation of $AsBr_2F$ to $AsBr_3$ and AsF_3 (eq 4).[43] It

$$[AsBr_4][AsF_6] \rightarrow [AsBr_4][F] + AsF_5 \quad (1)$$

$$[AsBr_4][F] \rightarrow AsBr_2F + Br_2 \quad (2)$$

$$AsBr_2F + AsF_5 \rightarrow 2AsF_3 + Br_2 \quad (3)$$

$$3AsBr_2F \rightarrow 2AsBr_3 + AsF_3 \quad (4)$$

has been shown that stoichiometric mixtures of $AsBr_3$, $AlBr_3$, and Br_2 in the ratios 1:1:1 and 1:2:1 also give rise to the $AsBr_4^+$ salts, which contain the $AlBr_4^-$ anion and possibly the $Al_2Br_7^-$ anion.[43] The bromoaluminate salts are markedly more stable than the AsF_6^- salt, surviving briefly as liquids at temperatures as high as 45 °C. The AsI_4^+ cation has been synthesized as the $AlCl_4^-$ salt by reaction of ICl with AsI_3 and $AlCl_3$ in anhydrous HCl at −95 to −78 °C.[42] The salt is highly unstable and has only been characterized at −110 °C by Raman spectroscopy.

The present investigation grew out of our earlier synthesis and stabilization of the $SbBr_4^+$ cation using the weakly coordinating anion $Sb(OTeF_5)_6^-$ as the counterion[30] and extends the use of such weakly coordinating anions to the formation of $AsBr_4^+$ salts, with the view of providing a fuller structural characterization of the $AsBr_4^+$ cation in the solid state by Raman spectroscopy and X-ray crystallography and in solution by ^{75}As NMR spectroscopy. The syntheses and characterization of the related $AsCl_4^+$ salts are also reported along with the first solution ^{75}As NMR study of the $AsCl_4^+$ cation. Density functional theory calculations have been used to predict the geometrical and vibrational parameters for all known and presently unknown PnX_4^+ (Pn = P, As, Sb, Bi) cations.

Results and Discussion

Syntheses and NMR Spectra of $[AsX_4][As(OTeF_5)_6]$ (X = Cl, Br), $[AsBr_4][AsF(OTeF_5)_5]$, and $[AsCl_4][Sb(OTeF_5)_{6-n}Cl_n]$. The $AsCl_4^+$ and $AsBr_4^+$ salts of the $As(OTeF_5)_6^-$ and $AsF(OTeF_5)_5^-$ anions were prepared by the reaction of $As(OTeF_5)_5$ and $AsF(OTeF_5)_4$ with stoichiometric amounts of $AsCl_3$ and $ClOTeF_5$ at room temperature and $AsBr_3$ and $BrOTeF_5$ at 0 °C in SO_2ClF solvent (eqs 5 and 6). The sample

$$AsX_3 + XOTeF_5 + As(OTeF_5)_5 \xrightarrow{\text{room temp}} [AsX_4][As(OTeF_5)_6] \quad (5)$$

$$AsBr_3 + BrOTeF_5 + AsF(OTeF_5)_4 \rightarrow [AsBr_4][AsF(OTeF_5)_5] \quad (6)$$

of $AsF(OTeF_5)_4$ used in this work contained ca. 5−10 mol % $As(OTeF_5)_5$ and resulted in the formation of the more stable $[AsBr_4][As(OTeF_5)_6]$ salt as a minor product in admixture with $[AsBr_4][AsF(OTeF_5)_5]$.

The $AsF(OTeF_5)_5^-$ anion is readily crystallized as the $AsBr_4^+$ salt (see X-ray crystal structure section) and has been observed in SO_2ClF solutions of $[AsBr_4][AsF(OTeF_5)_5]$ at −70 °C (F-on-As, −12.1 ppm, $\Delta\nu_{1/2}$ = 150 Hz). AB_4 patterns of the axial and equatorial $OTeF_5$ groups severely overlap each other and are in the range −40 to −43.5 ppm (A part) and −43.5 to −45.5 ppm (B part); the weak, severe AB_4 pattern of $As(OTeF_5)_6^-$ is centered at −42.4 ppm (−42.4 (A) and −42.0 (B) ppm for $[N(CH_3)_4][As(OTeF_5)_6]$ in SO_2ClF at 30 °C).[48] When either solution or solid samples of $[AsBr_4][AsF(OTeF_5)_5]$ are warmed, bromine is liberated (intense Raman band at 297 and 303 cm^{-1} at −113 °C). The room-temperature decomposition of $[AsBr_4][AsF(OTeF_5)_5]$ in SO_2ClF solvent has been monitored by ^{19}F NMR spectroscopy and occurs considerably more rapidly than that of $[AsBr_4][As(OTeF_5)_6]$, with the $AsF(OTeF_5)_5^-$ salt decomposing within 1 min and the $As(OTeF_5)_6^-$ salt requiring several hours to decompose at room temperature. The room-temperature decomposition of $[AsBr_4][As(OTeF_5)_6]$ was also monitored by ^{75}As NMR spectroscopy (see ^{75}As NMR section), and because all arsenic containing decomposition products have local symmetries at ^{75}As that result in rapid quadrupolar relaxation of the allowed ^{75}As nuclear spin transitions, their ^{75}As resonances are too broad to be observed. Only the highly symmetrical $AsBr_4^+$ and $As(OTeF_5)_6^-$ ions have sufficiently long relaxation times and correspondingly narrow line widths to be observed. The decomposition study of $[AsBr_4][As(OTeF_5)_6]$ showed that the cation and anion intensities decreased at the same rate. These findings are consistent with an initial decomposition step that is analogous to that proposed for the thermally less stable $[AsBr_4][AsF_6]$ salt (eq 1) and likely

(27) Miller, H. B.; Baird, H. W.; Bramlett, C. L.; Templeton, W. K. *J. Chem. Soc., Chem. Commun.* **1972**, 262.
(28) Müller, U. *Z. Naturforsch.* **1979**, *34B*, 681.
(29) Birchall, T.; Ballard, J. G. *Can. J. Chem.* **1978**, *56*, 2947.
(30) Casteel, W. J., Jr.; Kolb, P.; LeBlond, N.; Mercier, H. P. A.; Schrobilgen, G. J. *Inorg. Chem.* **1996**, *35*, 929 and references therein.
(31) Kolditz, L. *Z. Anorg. Allg. Chem.* **1955**, *280*, 313.
(32) Dess, H. M.; Parry, R. W.; Vidale, G. L. *J. Am. Chem. Soc.* **1956**, *78*, 5730.
(33) Kolditz, L. *Z. Anorg. Allg. Chem.* **1957**, *289*, 128.
(34) Seppelt, K.; Lentz, D.; Eysel, H.-H *Z. Anorg. Allg. Chem.* **1978**, *439*, 5.
(35) Kolditz, L.; Schmidt, W. *Z. Anorg. Allg. Chem.* **1958**, *296*, 188.
(36) Weidlein, J.; Dehnicke, K. *Z. Anorg. Allg. Chem.* **1965**, *337*, 113.
(37) Brinkmann, F. J.; Gerding, H.; Olie, K. *Recl. Trav. Chim. Pays-Bas* **1969**, *88*, 1358.
(38) Ballard, J. G.; Birchall, T. *Can. J. Chem.* **1978**, *56*, 2947.
(39) Demiray, A. F.; Brockner, W. *Monatsh. Chem.* **1979**, *110*, 799.
(40) Demircan, B.; Brockner, W. *Z. Naturforsch. A* **1983**, *38*, 811.
(41) Klapötke, T.; Passmore, J.; Awere, E. G. *J. Chem. Soc., Chem. Commun.* **1988**, 1426.
(42) Tornieporth-Oetting, I.; Klapötke, T. *Angew. Chem., Int. Ed. Engl.* **1989**, *28*, 1671.
(43) Klapötke, T.; Passmore, J. *J. Chem. Soc., Dalton Trans.* **1990**, 3815.
(44) Broschag, M.; Klapötke, T.; Tornieporth-Oetting, I. *J. Chem. Soc., Chem. Commun.* **1992**, 446.
(45) Preiss, H. *Z. Anorg. Allg. Chem.* **1971**, *380*, 71.
(46) Preiss, H. *Z. Anorg. Allg. Chem.* **1971**, *380*, 45.
(47) Minkwitz, R.; Nowicki, J.; Borrmann, H. *Z. Anorg. Allg. Chem.* **1991**, *596*, 93.
(48) Mercier, H. P. A.; Sanders, J. C. P.; Schrobilgen, G. J. *J. Am. Chem. Soc.* **1994**, *116*, 2921.

involves transfer of an $OTeF_5$ group from $As(OTeF_5)_6^-$ to the $AsBr_4^+$ cation to form an ion pair $[AsBr_4][OTeF_5]$ or Br_4-$AsOTeF_5$ as an intermediate (eq 7). Elimination of Br_2 and ligand redistribution on As^{III} leads to Br_2 and $As(OTeF_5)_3$ as the major decomposition products (eqs 8 and 9). Because $As(OTeF_5)_3$ is common to the decompositions of both $[AsBr_4][As(OTeF_5)_6]$ and the dominant $[AsBr_4][AsF(OTeF_5)_5]$ salts (vide infra), the $As(OTeF_5)_3$ resulting from eq 9 is masked in the ^{19}F NMR spectrum and must be inferred.

$$[AsBr_4][As(OTeF_5)_6] \rightarrow [AsBr_4][OTeF_5] + As(OTeF_5)_5 \quad (7)$$

$$[AsBr_4][OTeF_5] \rightarrow AsBr_2(OTeF_5) + Br_2 \quad (8)$$

$$AsBr_2(OTeF_5) + As(OTeF_5)_5 \rightarrow 2As(OTeF_5)_3 + Br_2 \quad (9)$$

When an SO_2ClF solution of $[AsBr_4][AsF(OTeF_5)_5]$ is warmed to room temperature, two new AB_4 patterns rapidly grew in and are assigned to $AsF(OTeF_5)_2$ and $As(OTeF_5)_3$. The latter product was confirmed by comparison with the ^{19}F NMR spectrum of an authentic sample obtained under the same solvent conditions at 29 °C (F_A, −45.2 ppm; F_B, −36.8 ppm; $^2J(^{19}F_A-^{19}F_B)$, 182 Hz; $^1J(^{125}Te-^{19}F_B)$, 3665 Hz; $^1J(^{125}Te-^{19}F_A)$, 3573 Hz). The formation of $AsF(OTeF_5)_2$ was confirmed by the observation of a singlet at −40.2 ppm accompanied by ^{125}Te satellites arising from $^3J(^{125}Te-^{19}F)$ (56 Hz) with its corresponding AB_4 pattern at −43.7 (A) and −37.9 (B) ppm; ($^2J(^{19}F_A-^{19}F_B)$, 186 Hz; $^1J(^{125}Te-^{19}F_B)$, 3674 Hz). The observed products are attributed to the decomposition of $[AsBr_4][AsF(OTeF_5)_5]$ according to eqs 10−12, which is analogous to the decomposition scheme proposed for $[AsBr_4][AsF_6]$ (eq 1−3).

$$[AsBr_4][AsF(OTeF_5)_5] \rightarrow [AsBr_4][F] + As(OTeF_5)_5 \quad (10)$$

$$[AsBr_4][F] \rightarrow AsBr_2F + Br_2 \quad (11)$$

$$AsBr_2F + As(OTeF_5)_5 \rightarrow AsF(OTeF_5)_2 + As(OTeF_5)_3 + Br_2 \quad (12)$$

The competing disproportionation of the intermediate, $AsBr_2F$ (eqs 11 and 12), to $AsBr_3$ and AsF_3, proposed in the decomposition scheme of $[AsBr_4][AsF_6]$ (eq 4), was not observed in the case of $[AsBr_4][AsF(OTeF_5)_5]$; i.e., no ^{19}F signal corresponding to AsF_3 was observed in the NMR spectrum of the decomposed solution and $AsBr_3$ was not observed in the low-temperature Raman spectrum of the decomposed solid sample.

In contrast, solutions of the $AsCl_4^+$ salt in SO_2ClF and the solid are stable indefinitely at room temperature. The ^{19}F NMR spectrum of $[AsCl_4][As(OTeF_5)_6]$ in SO_2ClF at 30 °C displays an intense, but severe, AB_4 pattern centered at −41.9 ppm, which is in good agreement with the previously reported value.[48]

Because the precursor to the $Sb(OTeF_5)_6^-$ anion, $Sb(OTeF_5)_5$, is unstable,[49] a synthetic route analogous to that used for $[AsCl_4][As(OTeF_5)_6]$ could not be used. The proposed alternative route involved a three-step scheme:

$$SbCl_5 + 6[Ag][OTeF_5] \xrightarrow{SO_2ClF} [Ag][Sb(OTeF_5)_6] + 5AgCl \quad (13)$$

$$AsCl_3 + [Ag][Sb(OTeF_5)_6] \xrightarrow{SO_2ClF} [AsCl_2][Sb(OTeF_5)_6] + AgCl \quad (14)$$

$$[AsCl_2][Sb(OTeF_5)_6] + Cl_2 \xrightarrow{X} [AsCl_4][Sb(OTeF_5)_6] \quad (15)$$

Rather, the interaction of $SbCl_5$ with $[Ag][OTeF_5]$ in SO_2ClF solvent yielded the mixed salts $[Ag][Sb(OTeF_5)_{6-n}Cl_n]$ (eq 16) (see Experimental Section for details of spectroscopic characterization), and no evidence was obtained for the formation of the $AsCl_2^+$ cation according to eq 14. Moreover, the ^{75}As NMR spectrum (recorded at 30 °C in SO_2ClF; see ^{75}As NMR spectroscopy section) and the solid-state Raman spectrum (see section on Raman spectroscopy of $AsBr_4^+$ and $AsCl_4^+$ salts) showed that the product of the reaction between $AsCl_3$ and $[Ag][Sb(OTeF_5)_{6-n}Cl_n]$ was an $AsCl_4^+$ salt (eq 17). The ^{121}Sb NMR spectrum of the product (eq 17) in SO_2ClF solvent at 30 °C failed to provide evidence for the mixed Sb^{III} and Sb^V anions because their low symmetries (high electric field gradients at the ^{121}Sb nuclei) are expected to lead to rapid quadrupolar relaxation. The ^{121}Sb NMR spectrum, however, confirmed the presence of the $Sb(OTeF_5)_6^-$ anion, which gave a broad singlet at 14.0 ppm ($\Delta\nu_{1/2} = 1040$ Hz), in agreement with the previously reported value (13.9 ppm in CH_3CN solvent at 30 °C).[48] The oxidation of As^{III} to As^V under these circumstances may be attributable to the incomplete reaction of $SbCl_5$ with $[Ag][OTeF_5]$ in SO_2ClF solvent (eq 16), leading to mixed $Sb(OTeF_5)_{6-n}Cl_n^-$ ($n \geq 0$) anions capable of oxidizing As^{III} to As^V in the absence of Cl_2 (eq 17). The observation of a band at 832 cm^{-1} in the product mixture is characteristic of the Te−O stretching frequency of the unreacted $OTeF_5^-$ anion, which occurs at 794 (Raman) and 806 (IR) cm^{-1} in unsolvated and strongly ion-paired $AgOTeF_5$ [50] and which rises to 868 and 867 cm^{-1} in the weakly ion-paired $N(CH_3)_4^+$ [51] and $N(n\text{-}Bu)_4^+$ [52] salts, respectively. Intermediate Te−O frequencies have been observed for the solvated metal cation salts.[50,53] The high frequency of the Te−O stretch in the initial product mixture (eq 16) is likely the result of long contacts between Ag^+ ions and oxygens/fluorines of the $OTeF_5$ groups of the mixed $Sb(OTeF_5)_{6-n}Cl_n^-$ anions. Addition of excess Cl_2 to the final product mixture (eqs 18 and 19) followed by removal of volatile materials under vacuum resulted in retention of the Raman spectrum of $AsCl_4^+$ and the growth of four medium to strong intensity Raman bands in the Sb−Cl stretching (280 and 331

$$SbCl_5 + 6[Ag][OTeF_5] \xrightarrow{SO_2ClF} [Ag][Sb(OTeF_5)_{6-n}Cl_n] + (6-n)AgCl + n[Ag][OTeF_5] \quad (n \geq 0) \quad (16)$$

$$AsCl_3 + 2[Ag][Sb(OTeF_5)_{6-n}Cl_n] \xrightarrow{SO_2ClF} Ag^+ + AsCl_4^+ + Sb(OTeF_5)_{6-n}Cl_{n-2}^- + Sb(OTeF_5)_{6-n}Cl_n^- + AgCl \quad (n \geq 2) \quad (17)$$

(49) Sanders, J. C. P.; Schrobilgen, G. J. Unpublished results.

(50) Colsman, M. R.; Newbound, T. D.; Marshall, L. J.; Noirot, M. D.; Miller, M. M.; Wulfsberg, G. P.; Frye, J. S.; Anderson, O. P.; Strauss, S. H. *J. Am. Chem. Soc.* **1990**, *112*, 2349.
(51) Christe, K.; Dixon, D. A.; Sanders, J. C. P.; Schrobilgen, G. J.; Wilson, W. W. *Inorg. Chem.* **1993**, *32*, 4089.
(52) Miller, P. K.; Abney, K. D.; Rappé, A. K.; Anderson, O. P.; Strauss, S. H. *Inorg. Chem.* **1988**, *27*, 2255.
(53) Kropshofer, H.; Leitzke, O.; Peringer, P.; Sladky, F. *Chem. Ber.* **1981**, *114*, 2644.

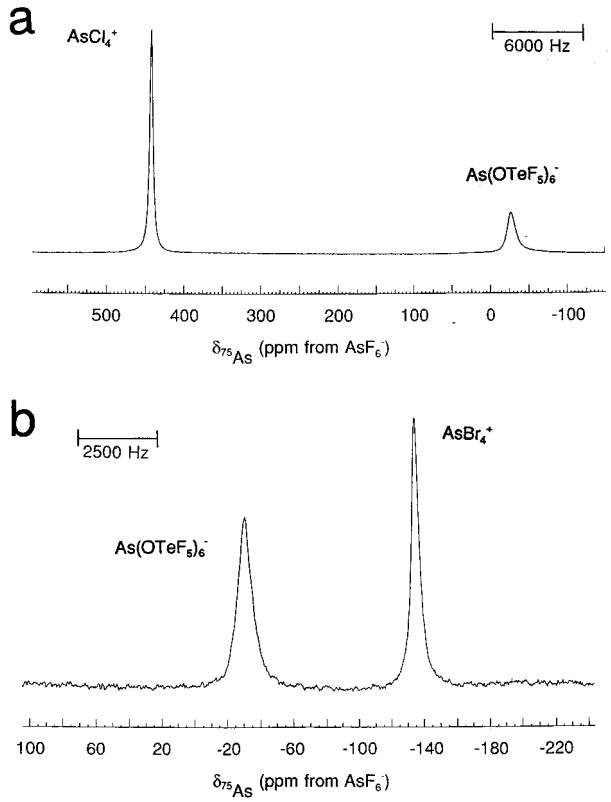

Figure 1. ^{75}As spectra of (a) $[AsCl_4][As(OTeF_5)_6]$ and (b) $[AsBr_4][As(OTeF_5)_6]$.

cm^{-1}) and Cl−Sb−Cl bending (164 and 190 cm^{-1}) regions, with the band at 331 cm^{-1} appearing as the most intense line in the spectrum. The bands are in good agreement with the

$$[Ag/AsCl_4][Sb(OTeF_5)_{6-n}Cl_{n-2}]_{(s)} + Cl_{2(l)} \rightarrow [Ag/AsCl_4][Sb(OTeF_5)_{6-n}Cl_n]_{(s)} \quad (n \geq 2) \quad (18)$$

$$[Ag][OTeF_5]_{(s)} + Cl_{2(l)} \rightarrow AgCl_{(s)} + ClOTeF_{5(l)} \quad (19)$$

frequencies reported for $SbCl_6^-$ and $SbCl_4^-$ [54] and likely arise from mixed Sb^V anions, $Sb(OTeF_5)_{6-n}Cl_n^-$. The band associated with the Te−O stretch of unreacted $OTeF_5$ vanished as a result of Cl_2 oxidation (eq 19), and $ClOTeF_5$ was identified as one of the volatile products. The reaction of excess Cl_2 with $AgOTeF_5$ was shown, in a separate experiment, to yield $ClOTeF_5$ (−70 °C in SO_2ClF; $^{19}F_A$, −46.1 ppm; $^{19}F_B$, −51.0 ppm; $^2J(^{19}F_A-^{19}F_B)$, 176 Hz; $^1J(^{125}Te-^{19}F_B)$, 3744 Hz; 50% of total intensity) and two other AB_4 patterns (−70 °C in SO_2ClF; $^{19}F_A$, −49.3 ppm; $^{19}F_B$, −53.9 ppm; $^2J(^{19}F_A-^{19}F_B)$, 175 Hz; $^1J(^{125}Te-^{19}F_B)$, 3859 Hz; 33% of total intensity; and $^{19}F_A$, −43.6 ppm; $^{19}F_B$, −47.9 ppm; $^2J(^{19}F_A-^{19}F_B)$, 178 Hz; 17% of total intensity) as volatile products.

^{75}As NMR Spectroscopy of $[AsX_4][As(OTeF_5)_6]$ (X = Cl, Br) and $[AsBr_4][AsF(OTeF_5)_5]$. The NMR spectra of the quadrupolar ^{75}As ($I = {}^3/_2$, 100%) nuclei in $[AsX_4][As(OTeF_5)_6]$ recorded in SO_2ClF solvent at 30 °C are depicted in Figure 1. As noted above, it was possible to record only the ^{75}As NMR spectrum of $[AsBr_4][As(OTeF_5)_6]$ and monitor its decomposition in mixtures with $[AsBr_4][AsF(OTeF_5)_5]$ because of the rapid room-temperature decomposition of the latter salt and failure of the low-symmetry arsenic-containing decomposition products to give ^{75}As resonances of sufficiently narrow line widths to be observed. Two relatively narrow signals were observed at 441.7 ppm ($\Delta\nu_{1/2} = 267$ Hz) and −28.7 ppm ($\Delta\nu_{1/2} = 618$ Hz) for $[AsCl_4][As(OTeF_5)_6]$ and at −29.2 ppm ($\Delta\nu_{1/2} = 513$ Hz) and −134.3 ppm ($\Delta\nu_{1/2} = 279$ Hz) for $[AsBr_4][As(OTeF_5)_6]$, with integrated relative intensities of cation/anion = 1:1. The signals at −29 ppm are assigned to the $As(OTeF_5)_6^-$ anion by comparison with the known $[N(CH_3)_4][As(OTeF_5)_6]$ salt (−29.1 ppm in CH_3CN at 30 °C),[48] and the remaining signals are assigned to the $AsCl_4^+$ and $AsBr_4^+$ cations, respectively. The chemical shift of $AsCl_4^+$ is the most deshielded ^{75}As chemical shift reported to date and exceeds that of aqueous Na_3AsO_4, for which a chemical shift of 369 ppm ($\Delta\nu_{1/2} = 989$ Hz) has been reported.[55,56] The observation of two relatively narrow signals in the ^{75}As NMR spectrum is consistent with the high symmetries about the ^{75}As atoms and low electric field gradients at the ^{75}As nuclei (see section on ^{75}As NMR relaxation). Slow decomposition of $[AsBr_4][As(OTeF_5)_6]$ was observed at 30 °C with the anion and the cation decomposing at approximately the same rate (see sections on synthesis of AsX_4^+ salts *and* ^{75}As NMR relaxation study).

Table 1. ^{75}As Spin−Lattice Relaxation Times (T_1) and Line Widths ($\Delta\nu_{1/2}$) for $[AsX_4][As(OTeF_5)_6]$ (X = Cl, Br)

	$T_1(^{75}As)$ [ms]	$\Delta\nu_{1/2,calc}$ [Hz][a]	$\Delta\nu_{1/2,obs}$ [Hz][b]
$AsCl_4^+$	1.367[c]/1.689[d]	233/188	267
$As(OTeF_5)_6^-$	0.692[c]/0.836[d]	460/381	618
$AsBr_4^+$	1.968[d]	162	279
$As(OTeF_5)_6^-$	1.027[d]	310	513

[a] Line width calculated from $\Delta\nu_{1/2} = (\pi T_1)^{-1}$. [b] Line width at half-height measured from the spectrum. [c] T_1 obtained by exponential fitting. [d] T_1 obtained from a semilogarithmic plot.

The spin−lattice relaxation times (T_1) have been determined for the ^{75}As environments of $[AsBr_4][As(OTeF_5)_6]$ and $[AsCl_4][As(OTeF_5)_6]$ in SO_2ClF solutions at 30 °C using the standard inversion−recovery sequence (Table 1 and Supporting Information) and are the first such studies for tetrahedrally coordinated arsenic. The spin−lattice relaxation times obtained from $\ln(I_\infty - I_\tau)$ versus τ plots are generally found to be longer than those derived from the more accurate exponential fitting (τ and I_τ denote the delay time and the signal intensity using the delay time τ in the inversion−recovery pulse sequence, $\pi-\tau-{}^{\pi}/_2-$acquisition).

The quadrupolar relaxation mechanism for ^{75}As (100% natural abundance, $I = {}^3/_2$) is dominant and gives rise to short spin−lattice relaxation times. The $AsBr_4^+$ cation has a shorter T_1 value than the $AsCl_4^+$ cation because the ionic radius of $AsBr_4^+$ is larger, resulting in a longer molecular correlation time, τ_c. The $As(OTeF_5)_6^-$ anion was found to have a shorter ^{75}As spin−lattice relaxation time than either $AsCl_4^+$ or $AsBr_4^+$, as is evident in the ^{75}As NMR spectra (Figure 1), where the anion signal is broader than that of either cation. The additional line broadening results from the larger radius of the $As(OTeF_5)_6^-$ anion and its correspondingly longer rotational correlation time. An ^{75}As T_1 value of 2.99 ms was previously reported for $[N(CH_3)_4][As(OTeF_5)_6]$ in CH_3CN solution at 30 °C. This value is 3−4 times longer than the values obtained in the present study for the anions of $[AsBr_4][As(OTeF_5)_6]$ and $[AsCl_4][As(OTeF_5)_6]$ in SO_2ClF solvent at 30 °C. The differences are likely related to the higher viscosity and lower polarity of SO_2ClF solvent, with the latter favoring ion pair formation, and with both increased ion pairing and higher viscosity serving to increase τ_c and, hence,

(54) Nakamoto, K. In *Infrared and Raman Spectra of Inorganic and Coordination Compounds*, 5th ed.; J. Wiley & Sons: New York, 1997; Part A, Chapter II, pp 198 and 216 and references therein.

(55) Balimann, G.; Pregosin, P. S. *J. Magn. Reson.* **1977**, *26*, 283.
(56) McGarvey, G. B.; Moffat, J. B. *J. Magn. Reson.* **1990**, *88*, 305.

Table 2. Summary of Crystal Data and Refinement Results for $[AsCl_4][As(OTeF_5)_6]$ and $[AsBr_4][AsF(OTeF_5)_5]$

	$[AsCl_4][As(OTeF_5)_6]$		$[AsBr_4][AsF(OTeF_5)_5]$
formula	$As_2Cl_4F_{30}O_6Te_6$	$As_2Cl_4F_{30}O_6Te_6$	$As_2Br_4F_{26}O_5Te_5$
space group (No.)	$R\bar{3}$ (148)	$R\bar{3}$ (148)	$P\bar{1}$ (2)
temp (°C)	−123	−183	−183
a (Å)	9.8741(14)	19.688(3)	9.778(4)
b (Å)	9.8741(14)	19.688(3)	17.731(7)
c (Å)	55.301(11)	55.264(11)	18.870(8)
α (deg)	90.00	90.00	103.53(4)
β (deg)	90.00	90.00	103.53(4)
γ (deg)	120.00	120.00	105.10(4)
V (Å^3)	4669(1)	18552(5)	2915(2)
Z	6	24	4
λ (Å)	0.710 73	0.710 73	0.710 73
ρ_{calcd} (g cm^{-3})	3.677	3.702	3.831
μ (mm^{-1})	8.20	8.26	12.863
R_1[a]	0.0438	0.1341	0.0368
wR_2[b]	0.1445	0.4246	0.0513

[a] $R_1 = (\sum||F_o| - |F_c||)/\sum|F_o|$ for $I > 2\sigma(I)$. [b] $wR_2 = [\sum[w(F_o^2 - F_c^2)^2]/\sum w(F_o^2)^2]^{1/2}$ for $I > 2\sigma(I)$.

T_1. A similar solvent effect was found for AsR_4^+ cations, where a broadening of the ^{75}As resonance was observed on going from H_2O to DMSO solvent.[55,56]

X-ray Crystal Structures of $[AsCl_4][As(OTeF_5)_6]$ (−123 and −183 °C) and $[AsBr_4][AsF(OTeF_5)_5]$ (−183 °C). Details of the data collection parameters and other crystallographic information are given in Table 2. Important bond lengths and angles for the AsX_4^+ cations (X = Cl, Br), together with average bond lengths and angles for the $As(OTeF_5)_6^-$ and $AsF(OTeF_5)_5^-$ anions, are listed in Table 3. The bond valences for individual bonds in the cations and for their long contacts as defined by Brown are also included in Table 3. The geometrical parameters (bond lengths, angles, contacts) of both the high-temperature and low-temperature phases of $[AsCl_4][As(OTeF_5)_6]$ are essentially identical; consequently, the numerical values for the structure at −123 °C are reported in parentheses, and those for the −183 °C structure are given in square brackets.

(a) $[AsCl_4][As(OTeF_5)_6]$. The structures of the $AsCl_4^+$ cation and $As(OTeF_5)_6^-$ anion have been reported previously in $[AsCl_4][AsF_6]$[46,47] and $[AsCl_4][SbCl_6]\cdot AsCl_3$[45] and in $[N(CH_3)_4][As(OTeF_5)_6]$.[48] The compound $[AsCl_4][As(OTeF_5)_6]$ consists of well-separated $AsCl_4^+$ cations and $As(OTeF_5)_6^-$ anions (Figure 2). In this structure and in the crystal structure of $[N(CH_3)_4][As(OTeF_5)_6]$, the central arsenic atom is octahedrally coordinated to the six oxygen atoms and each of the six tellurium atoms is octahedrally coordinated to an oxygen and five fluorines so that each anion can be described as an octahedron of octahedra. The $As(OTeF_5)_6^-$ anions in the present structure display features in common with the two crystallographically nonequivalent $Sb(OTeF_5)_6^-$ anions in $[SbX_4][Sb(OTeF_5)_6]$ (X = Cl, Br).[30] While the $AsCl_4^+$ cations are ordered at −123 and −183 °C and have the expected tetrahedral geometry, one [two] of the two [four] crystallographically independent anions is-[are] perfectly ordered and the other[s] suffers from an orientational disorder (Figure 3). The degree of disorder is lower at −183 °C than at −123 °C, which is expected for a phase transition that occurs at −155 °C. This disorder can be described as the superposition of four (two) anions where the As and Te atoms occupy the same positions; their respective thermal parameters are as low as those observed in the nondisordered anions. In contrast to the anions in $[SbX_4][Sb(OTeF_5)_6]$, where both fluorine and oxygen positions are distinguishable, only the oxygen positions could be resolved in the present structure (see Experimental Section).

The average As−O distances (1.79(1) Å) [1.801(6) Å] of the $As(OTeF_5)_6^-$ anion are comparable to the average As^V−O distances observed for hexacoordinate As^V in $[N(CH_3)_4][As(OTeF_5)_6]$ (1.807 Å)[48] and $M_2(As_2F_{10}O)\cdot H_2O$ (for M = Rb, As−O = 1.75 Å; for M = K, As−O = 1.74 Å).[58] The average Te−O (1.85(1) Å) [1.85(1) Å] and Te−F (1.81(1) Å) [1.80(1) Å] bond distances are comparable to those found in many other $OTeF_5$ compounds. The As−O−Te angles are very similar to those reported previously for $[N(CH_3)_4][As(OTeF_5)_6]$ (140(2)°).[48]

The As^V−Cl bond lengths of $AsCl_4^+$ are identical within 3σ, and the average Cl−As−Cl angles are close to the ideal tetrahedral value. The structural parameters of the $AsCl_4^+$ cation are in agreement with those previously reported ($[AsCl_4][AsF_6]$, As−Cl, 2.0545(9) Å and Cl−As−Cl, 108.03(5)°, 110.20(3)°;[47] $[AsCl_4][SbCl_6]\cdot AsCl_3$, As−Cl, 2.03(2)−2.07(2) Å).[45] Each cation in $[AsCl_4][As(OTeF_5)_6]$ has three long As···F contacts with three fluorine atoms belonging to three different ordered anions (As(1)···F(2), 3.413(4) Å × 3) [As(2)···F(20), 3.377(7) Å × 3, and As(1)···F(5,7,12), 3.411(7), 3.447(7), 3.432(7) Å] that pass through the centers of three of the faces of the tetrahedron (those containing the halogen atom positioned on the C_3 axis (Cl(2)) [Cl(6)]), whereas the face containing the three symmetry-related halogen atoms (Cl(1)) [Cl(5)] does not have any long As···F contacts (Figure 2). In the −183 °C structure, one of the cations is no longer positioned on a C_3 axis but still maintains three long anion−cation contacts (As(1)). In the previously reported structure of $[AsCl_4][AsF_6]$,[47] the $AsCl_4^+$ cation has four long F···$AsCl_4^+$ contacts, with each contacting fluorine approaching the center of one of the four faces of the $AsCl_4^+$ tetrahedron so that a regular tetrahedron of fluorines surrounds the $AsCl_4^+$ tetrahedron (3.445 Å × 4). Although the F···$AsCl_4^+$ distances to $AsCl_4^+$ in $[AsCl_4][As(OTeF_5)_6]$ are at the limit of the sum of the van der Waals radii (3.35 [59]−3.40 [60] Å), bond valence calculations indicate that these long contact interactions are weaker in the $As(OTeF_5)_6^-$ salt; i.e., the total bond valence for each arsenic atom of $AsCl_4^+$ is (4.955) [4.906, 5.013] v.u. (bond valence units), with contributions of (1.241−1.205) [1.255−1.208, 1.238−1.258] v.u./Cl atom and (0.009) [0.009, 0.008−0.009] v.u./long fluorine contact. The corresponding value for the AsF_6^- salt is 4.87 (1.210 v.u./Cl atom and 0.008 v.u./long fluorine contact). The more weakly coordinating character of the $As(OTeF_5)_6^-$ anion is reflected in the smaller number of long anion−cation contacts and in the smaller contribution to the total bond valence of the As atom of the cation (Table 3). The occurrence of contacts between the central atom of the cation and fluorines of the anion is also a feature encountered in the related $[SbCl_4][Sb(OTeF_5)_6]$[30] and $[SbCl_4][Sb_2F_{11}]$[27] salts where the Sb atom has three long Sb···F contacts at 3.346(2) Å and four long Sb···F contacts at 3.0 Å, respectively. Other anion−cation contacts occur between the halogen atoms and several fluorine atoms of both ordered and disordered anions that are at the limit of the Cl···F van der Waals distance (3.15 [59]−3.20 [60] Å), ranging from 3.022(9) to 3.312(5) Å (−123 °C) and 3.01(1) to 3.303(7) (−183 °C).

The crystal structure of $[AsCl_4][As(OTeF_5)_6]$ is dominated by the larger $As(OTeF_5)_6^-$ anions and consists of a hexagonal closest-packed anion lattice with the cations occupying what are formally octahedral interstitial sites which are, in fact, trigonal prismatic holes with three anions from each layer defining the site. Interestingly, the $AsCl_4^+$ cations are not located

(57) Brown, I. D. *J. Solid State Chem.* **1974**, *11*, 214.
(58) Haase, W. *Acta Crystallogr.* **1974**, *B30*, 1722.
(59) Bondi, A. *J. Phys. Chem.* **1964**, *68*, 441.
(60) Pauling, L. *The Nature of the Chemical Bond*, 3rd ed.; Cornell University Press: Ithaca, NY, 1960; p 260.

Table 3. Selected Bond Lengths (Å), Bond Valences (v.u.),[a] and Bond Angles (deg) in $[AsCl_4][As(OTeF_5)_6]$ (−123 and −183 °C) and $[AsBr_4][AsF(OTeF_5)_5]$

	$[AsCl_4][As(OTeF_5)_6]$ (−123 °C)		
As(1)−Cl(1)	2.045(2) × 3 [1.241 × 3]	As(1)−Cl(2)	2.056(3) [1.205]
As(1)···F	3.413(4) × 3 [0.009 × 3]		
total bond valence	As(1) 4.955		
Cl(1)#1-As(1)−Cl(1)	108.72(5) × 3	Cl(1)−As(1)−Cl(2)	110.21(5) × 3
	$[AsCl_4][As(OTeF_5)_6]$ (−183 °C)		
As(1)−Cl(2)	2.042(3) [1.251]	As(1)−Cl(1)	2.040(5) [1.258]
As(1)−Cl(3)	2.045(3) [1.241]	As(1)−Cl(4)	2.046(3) [1.238]
As(2)−Cl(5)	2.041(5) [1.255]	As(2)−Cl(6)	2.055(3) × 3 [1.208 × 3]
As(1)···F	3.411(7), 3.447(7), 3.432(7) [0.009, 0.008, 0.008]		
As(2)···F	3.377(7) × 3 [0.009 × 3]		
total bond valence	As(1) 5.013	As(2) 4.906	
Cl(2)−As(1)−Cl(1)	110.16(12)	Cl(2)−As(1)−Cl(3)	108.90(12)
Cl(1)−As(1)−Cl(3)	110.36(11)	Cl(2)−As(1)−Cl(4)	108.56(13)
Cl(1)−As(1)−Cl(4)	110.29(11)	Cl(3)−As(1)−Cl(4)	108.53(11)
Cl(5)−As(2)−Cl(6)	110.41(10)	Cl(6)#1-As(2)−Cl(6)	108.52(10)
	$[AsBr_4][AsF(OTeF_5)_5]$		
As(1)−Br(1)	2.233(2) [1.248]	As(2)−Br(5)	2.233(2) [1.248]
As(1)−Br(2)	2.235(2) [1.241]	As(2)−Br(6)	2.234(2) [1.245]
As(1)−Br(3)	2.233(2) [1.248]	As(2)−Br(7)	2.236(2) [1.238]
As(1)−Br(4)	2.227(2) [1.269]	As(2)−Br(8)	2.225(2) [1.275]
As(1)···F	3.826(7) [0.003]		
total bond valence	As(1) 5.009	As(2) 5.006	
Br(4)−As(1)−Br(3)	110.32(7)	Br(4)−As(1)−Br(1)	108.29(7)
Br(3)−As(1)−Br(1)	109.88(6)	Br(4)−As(1)−Br(2)	108.88(7)
Br(3)−As(1)−Br(2)	108.92(7)	Br(1)−As(1)−Br(2)	110.54(6)
Br(8)−As(2)−Br(5)	109.24(8)	Br(8)−As(2)−Br(6)	110.52(7)
Br(5)−As(2)−Br(6)	110.19(7)	Br(8)−As(2)−Br(7)	110.70(7)
Br(5)−As(2)−Br(7)	108.63(7)	Br(6)−As(2)−Br(7)	107.53(6)

[a] Bond valence units (v.u.) are defined in ref 57. $R_o = 2.125$ (As−Cl), $R_o = 1.65$ (As−F), $R_o = 2.315$ (As−Br) and $B = 0.37$ were used.

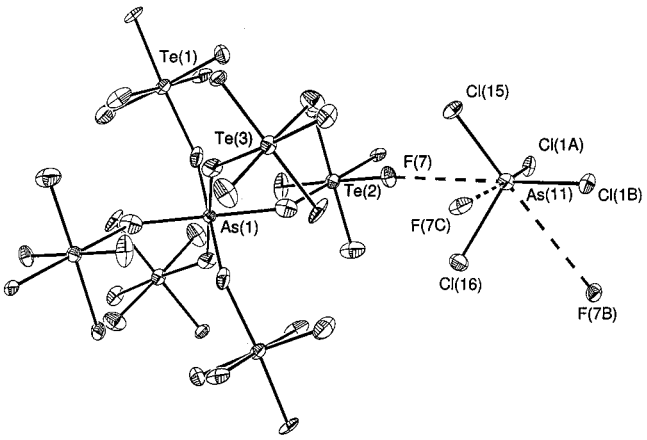

Figure 2. Geometry of the $AsCl_4^+$ cation and ordered $As(OTeF_5)_6^-$ anion at −183 °C. The coordination environment of the $AsCl_4^+$ cation with fluorine atoms of three different anions is denoted by dashed lines. Thermal ellipsoids are shown at the 50% probability level.

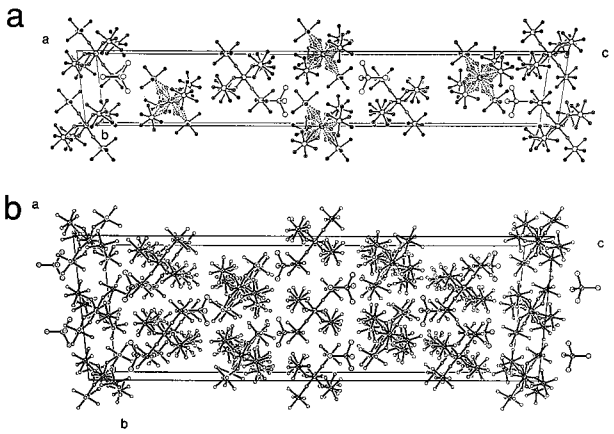

Figure 3. Packing of $[AsCl_4][As(OTeF_5)_6]$ at (a) −123 °C and at (b) −183 °C.

in the middle of the trigonal prismatic holes in either structure but are closer to the layer containing the nondisordered (As(1)) [As(1)−As(3)] anions than to the layer containing the disordered (As(5)) [As(2)−As(4)] anions. This displacement can be understood by considering the total bond valence around arsenic in the $AsCl_4^+$ cations. If the cations were positioned at the centers of the trigonal prismatic sites, the cations would have long As···F contacts with fluorines of both the disordered and nondisordered anions. The contacts would be too long to contribute to the total bond valence of (As(1)) [As(1), As(3)] so that the total bond valence of five for the (As(1)) [As(1), As(3)] atoms would not be met. It appears that the As···F contacts serve to constrain the ordered anion in one orientation, while the absence of contacts with the fluorines of the other anion account for the disorder on this anion. Similar behavior was previously encountered in the crystal structures of $[SbX_4][Sb(OTeF_5)_6]$ (X = Cl, Br).[30]

(b) $[AsBr_4][AsF(OTeF_5)_5]$. The structures of the $AsBr_4^+$ cation and $AsF(OTeF_5)_5^-$ anion are both reported for the first time. The $AsF(OTeF_5)_5^-$ anion is isovalent and isostructural with $TeF(OTeF_5)_5$, which has been characterized by ^{19}F NMR spectroscopy.[61] The compound consists of well-separated $AsBr_4^+$ cations and $AsF(OTeF_5)_5^-$ anions (Figure 4). The two crystallographically independent $AsBr_4^+$ cations have the expected tetrahedral geometry, with the Br−As−Br angles close to the ideal tetrahedral value (range: 107.53(6)−110.70(7)°). All the As^V−Br bond lengths are equal within 3σ, ranging from 2.225(2) to 2.236(2) Å, and are in excellent agreement with our previous empirically predicted value of 2.221 Å[30] and theoretical values (see Computational Results). The As^V−Br bond length reported

(61) Lentz, D.; Pritzkow, H.; Seppelt, K. *Inorg. Chem.* **1978**, *17*, 1926.

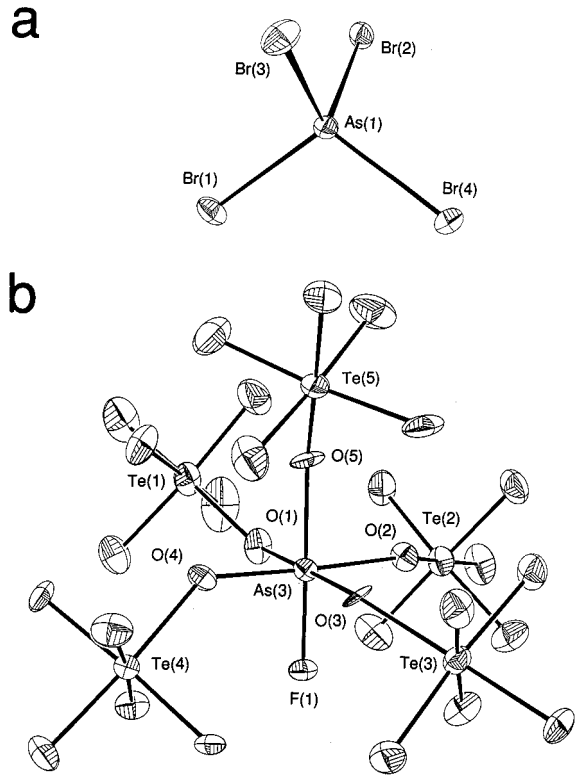

Figure 4. Geometries of the (a) $AsBr_4^+$ cation and (b) $AsF(OTeF_5)_5^-$ anion in $[AsBr_4][AsF(OTeF_5)_5]$ with thermal ellipsoids shown at the 50% probability level.

in this paper is presently the only As^V-Br bond length known, and as expected, it is shorter than the terminal $As^{III}-Br$ bond lengths observed in $AsBr_3$ (2.322(1) Å),[62] $As_2Br_8^{2-}$ (2.347(1)−2.387(1) Å),[63] and $[AsBr_4^-]_n$ (2.393(1) Å).[63]

The central As^V atom in the $AsF(OTeF_5)_5^-$ anion is coordinated to five crystallographically nonequivalent $OTeF_5$ groups and to a fluorine atom so that the gross geometry can be described as a pseudo-octahedron in which all the $OTeF_5$ groups of the anion have the pseudo-octahedral geometry observed in other $OTeF_5$ compounds (vide supra). The As^V-O (av 1.805(9) Å), $Te^{VI}-O$ (av 1.849(8) Å), and $Te^{VI}-F$ (av 1.827(9) Å) bond lengths are identical to those observed in $As(OTeF_5)_6^-$ (vide supra and Supporting Information), and the unique As^V-F (1.721(6) and 1.734(6) Å) bond length is equal, within 3σ, to the As^V-F bond length in the AsF_6^- anion.[64] It is worth noting that the As^V-O_{eq} and As^V-O_{ax} bond lengths are found to be equal, in contrast to the $Te^{IV}-O$ bond lengths in $Te(OTeF_5)_5^-$,[65] where the equatorial $Te^{IV}-O$ bonds were found to be longer than the axial $Te^{IV}-O$ bond. The difference presumably arises because the lone pair−equatorial Te−O bond pair repulsions in $Te(OTeF_5)_5^-$ are significantly greater than the As−F bond pair−equatorial Te−O bond pair repulsions in $AsF(OTeF_5)_5^-$. The latter appears to be very similar and is supported by the observation that the $O_{ax}-As-O_{eq}$ and $F-As-O_{eq}$ angles are all equal, within 3σ, to 90°, while in $Te(OTeF_5)_5^-$, the $O_{ax}-As-O_{eq}$ angles are compressed from the ideal 90° angle to an average angle of 81°.

(62) Schmidbaur, H.; Bublak, W.; Huber, B.; Müller, G. *Angew. Chem., Int. Ed. Engl.* **1987**, *26*, 234.
(63) Kaub, J.; Sheldrick, W. S. *Z. Naturforsch.* **1984**, *39b*, 1257.
(64) Zalkin, A.; Ward, D. L.; Biagioni, R. N.; Templeton, D. H.; Bartlett, N. *Inorg. Chem.* **1978**, *17*, 1318.
(65) Mercier, H. P. A.; Sanders, J. C. P.; Schrobilgen, G. J. *Inorg. Chem.* **1995**, *34*, 5261.

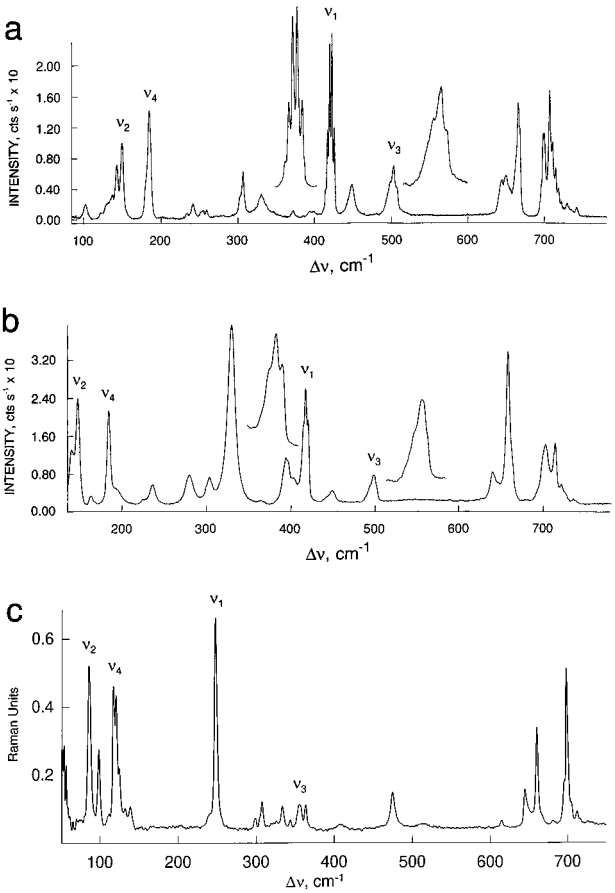

Figure 5. Raman spectra of microcrystalline (a) $[AsCl_4][As(OTeF_5)_6]$ (−124 °C), (b) $[Ag/AsCl_4][Sb(OTeF_5)_{6-n}Cl_n]$ (24 °C) recorded using 514.5 nm excitation, and (c) $[AsBr_4][AsF(OTeF_5)_5]$ (−110 °C) recorded using 1064 nm excitation. Labels $\nu_1-\nu_4$ denote cation bands. Enlargements show the natural abundance chlorine isotopic shifts on the ν_1-(A_1) and $\nu_3(T_2)$ bands.

As a consequence of the steric effects of the axial $OTeF_5$ group, the relative conformations of the equatorial $OTeF_5$ groups in $AsF(OTeF_5)_5^-$ are very similar to those in $Te(OTeF_5)_5^-$. The axial $OTe(5/10)F_5$ group points toward the equatorial $OTe(3/9)F_5$ group, which, in turn, is directed away from the $OTe(5/10)F_5$ group; the two $OTeF_5$ groups are, however, not perfectly eclipsed. The two equatorial *trans*-$OTeF_5$ groups, $OTe(2/8)F_5$ and $OTe(4/6)F_5$, are cis to $OTe(3/9)F_5$ and also point away from the apical $OTe(5/10)F_5$ group so that they adopt a trans, syn conformation relative to one another. The $OTe(1/7)F_5$ group trans to $OTe(3/9)F_5$ points toward the apical $OTe(5/10)F_5$ group so that these two equatorial groups have a trans, anti conformational relationship apparently imposed by $OTe(5/10)F_5\cdots OTe(3/9)F_5$ steric interactions.

The closest anion−cation contacts occur at 3.157(6) [F(1)···Br(1)], 3.530(6) [F(2)···Br(8)], and 3.346(6) [As(2)···F(71)] Å and are at the limit of the Br···F van der Waals distance (3.3 Å). Unlike the $AsCl_4^+$ structure, there are no $F\cdots AsBr_4^+$ anion−cation contacts (i.e., the total bond valence for each arsenic atom is 5.01 and 5.00 v.u., with contributions of 1.24−1.27 and 1.24−1.28 v.u./Br atom and where the shortest $F\cdots AsBr_4^+$ distance is 3.826(7) Å (As(1)···F(94)). Moreover, it is worth noting that there are no $(F_5TeO)_5As-F\cdots AsBr_4^+$ contacts, with the shortest distances at As(3)−F(1)···As(1) = 4.960 Å and As(4)−F(2)···As(2) = 5.422 Å.

Raman Spectra of $AsBr_4^+$ and $AsCl_4^+$ Salts. The solid-state Raman spectra of the title compounds are shown in Figure 5. The observed frequencies and their assignments are sum-

Table 4. Raman Frequencies and Assignments in $[AsCl_4][As(OTeF_5)_6]$, $[AsBr_4][AsF(OTeF_5)_5]$, $[Ag/AsCl_4][Sb(OTeF_5)_{6-n}Cl_{n-2}]$, and $[Ag/AsCl_4][Sb(OTeF_5)_{6-n}Cl_n]$ ($n \geq 2$)[a]

frequency, cm^{-1}				assignment	
$[AsCl_4][As(OTeF_5)_6]$	$[AsBr_4]$ $[AsF(OTeF_5)_5]$[b]	$[Ag/AsCl_4]$ $[Sb(OTeF_5)_{6-n}Cl_{n-2}/$ $Sb(OTeF_5)_{6-n}Cl_n]$[c]	$[Ag/AsCl_4]$ $[Sb(OTeF_5)_{6-n}Cl_n]$[d]	cation[e]	anion[f]
503(29)	356(12)	502(15)	499(17)	$\nu_3(T_2)$, ν_{as}	
	353(12)				
420(100)	247(100)	419(100)	419(65)	$\nu_1(A_1)$, ν_s	
186(59)	120(64)	185(83)	185(53)	$\nu_4(T_2)$, δ_{as}	
	116(68)				
151(41)	85(79)	146(63)	147(60)	$\nu_2(E)$, δ_s	
741(7)		736(10)	737(2)		$\nu_8(E)$, $\nu_{as}(TeF_4)$
729(9)			727(sh)		
			723(11)		
714(28)	712(8)		715(33)		$\nu_1(A_1)$, ν(TeF)
706(70)	705(sh)	700(61)	704(33)		
698(48)	699(76)		696(sh)		
	694(sh)				
664(64)	660(47)	660(68)	658(84)		$\nu_2(A_1)$, $\nu_s(TeF_4)$
649(24)	644(19)	645(sh)	647(sh)		$\nu_5(B_1)$, $\nu_{as}(TeF_4)$
643(21)			640(14)		
	614(5)				
	514(4)				
449(19)	473(18)	440(sh)	449(6)		$\nu_3(A_1)$, ν_s(Te−O)
			440(sh)		coupled with ν_s(M−O)
414(sh)	406(3)	395(43)	405(sh)		
400(5)			395(25)		
372(5)	362(12)		365(2)		
	342(5)				
331(14)	332(12)	332(24)	331(100)[g]		$\nu_9(E)$, $\delta(FTeF_4)$
307(26)	306(13)	305(24)	304(16)		$\nu_4(A_1)$, $\delta_s(FTeF_4)$
	297(6)		280(17)[g]		
243(9)	239(sh)	233(22)	237(11)		$\nu_{11}(E)$, $\delta_{as}(TeF_4)$
			226(sh)		
			190(sh)[g]		
			164(6)[g]		
144(30)	137(12)	139(54)	140(31)		τ(TeOM)
	131(11)				
	124(29)				
103(9)	110(sh)	106(10)			lattice mode
	97(38)	86(10)			

[a] Values in parentheses denote relative intensities and sh denotes a shoulder. [b] Contains 5−10 mol % $[AsBr_4][As(OTeF_5)_6]$. [c] Mixture derived from eq 17. An additional peak assigned to the Te−O stretching frequency of unreacted $OTeF_5^-$ was also observed at 832(4) cm^{-1}. [d] Mixture derived from eq 18. [e] The frequencies reported for $\nu_3(T_2)$ and $\nu_1(A_1)$ for $AsCl_4^+$ correspond to those of the $As^{35}Cl_2{}^{37}Cl_2^+$ and $As^{35}Cl_3{}^{37}Cl^+$ isotopomers, respectively. [f] The vibrational modes of the $OTeF_5$ groups are assigned under C_{4v} symmetry (see refs 33 and 51. [g] Assigned to Sb−Cl stretching (331 and 280 cm^{-1}) and Cl−Sb−Cl bending (190 and 164 cm^{-1}) modes; cf. ref 54.

marized in Table 4. The frequency assignments for the $OTeF_5$ groups of $AsF(OTeF_5)_5^-$, $As(OTeF_5)_6^-$, and $Sb(OTeF_5)_{6-n}Cl_n^-$/ $Sb(OTeF_5)_{6-n}Cl_{n-2}^-$ anions were made by comparison with the assignments for $[N(CH_3)_4][M(OTeF_5)_6]$ (M = As, Sb)[48] and require no further comment. In the case of the assignment of the As−F stretching mode of $[AsBr_4][AsF(OTeF_5)_5]$, no definitive assignment of this mode is possible because several bands arising from Te−F stretching motions also appear in the anticipated region (ca. 680−700 cm^{-1}) and are expected to be considerably more intense than the As−F stretch. The Sb−Cl stretching and Cl−Sb−Cl bending modes of the mixed Cl/ $OTeF_5$ antimony(V) anions have not been explicitly assigned, but bands that compare favorably with their counterparts in the $SbCl_4^-$ and $SbCl_6^-$ anions[54] are indicated in Table 4 (also see sections on syntheses and NMR spectra). The assignments of the $AsCl_4^+$ and $AsBr_4^+$ cation vibrations were made by comparison with the vibrational spectra of $[AsX_4][AsF_6]$ (X = Cl, Br),[36,41,43] $[AsCl_4][SbF_6]$,[38] $[AsCl_4][MCl_4]$ (M = Al, Ga),[40] and $[AsBr_4][Al_2Br_7]$[43] and were confirmed by theoretical calculations (see Computational Results and Table 6). Splittings arising from the $^{35/37}Cl$ isotope effect, which were not reported in previous studies, were, however, observed on $\nu_1(A_1)$ and $\nu_3(T_2)$ of the $AsCl_4^+$ cation for both the $As(OTeF_5)_6^-$ and $Sb(OTeF_5)_{6-n}Cl_n^-$ salts, although they were better resolved in

Table 5. Raman Frequencies and Assignments for the Chlorine Isotopic Splitting on $\nu_1(A_1)$ and $\nu_3(T_2)$ of $AsCl_4^+$ in $[Ag/AsCl_4][Sb(OTeF_5)_{6-n}Cl_n]$ and $[AsCl_4][As(OTeF_5)_6]$

assignment	frequencies, cm^{-1} Sb[a]	As[b]
$\nu_1(A_1)$ band		
$\nu_1(A_1)$, $As^{35}Cl_4^+$	421.4	423.0
$\nu_1(A_1)$, $As^{35}Cl_3{}^{37}Cl^+$	418.5	420.1
$\nu_1(A_1)$, $As^{35}Cl_2{}^{37}Cl_2^+$	416.0	417.2
$\nu_1(A_1)$, $As^{35}Cl^{37}Cl_3^+$	413.0	414.5
$\nu_1(A_1)$, $As^{37}Cl_4^+$	410.0	*c*
$\nu_3(T_2)$ band		
$\nu_3(T_2)$, $As^{35}Cl_4^+$; $\nu_4(E)$, $As^{35}Cl_3{}^{37}Cl^+$; $\nu_6(B_1)$, $As^{35}Cl_2{}^{37}Cl_2^+$	502.0	507.0
$\nu_2(A_1)$, $As^{35}Cl_3{}^{37}Cl^+$		
$\nu_2(A_1)$, $As^{35}Cl_2{}^{37}Cl_2^+$	499.0	503.0
$\nu_2(A_1)$, $As^{35}Cl^{37}Cl_3^+$	495.4	498.0
$\nu_3(T_2)$, $As^{37}Cl_4^+$; $\nu_4(E)$, $As^{35}Cl^{37}Cl_3^+$; $\nu_8(B_2)$, $As^{35}Cl_2{}^{37}Cl_2^+$	490.0	493.0

[a] Values observed for the $Sb(OTeF_5)_{6-n}Cl_n^-$ salt. [b] Values are for the $As(OTeF_5)_6^-$ salt. [c] Too weak to be observed.

Table 6. Calculated (LDFT/DZVP) and Experimental[a] Geometries and Vibrational Frequencies for the MX_4^+ Cations (M = P, As, Sb, Bi; X = F, Cl, Br, I)

Bond Distance (Å)							
PF_4^+	1.505 [1.480, 1.470]	AsF_4^+	1.666 [1.606]	SbF_4^+	1.870	BiF_4^+	1.917
PCl_4^+	1.967 [1.927(2)]	$AsCl_4^+$	2.089 [2.040(5)−2.056(3)]	$SbCl_4^+$	2.275 [2.221(2)]	$BiCl_4^+$	2.367
PBr_4^+	2.145 [2.17(1)]	$AsBr_4^+$	2.258 [2.225(2)−2.236(2)]	$SbBr_4^+$	2.426 [2.385(2)]	$BiBr_4^+$	2.506
PI_4^+	2.397 [2.396(9)]	AsI_4^+	2.498 [2.449]	SbI_4^+	2.660	BiI_4^+	2.750

	frequency (cm^{-1})[b]							
symmetry	PF_4^+		PCl_4^+		PBr_4^+		PI_4^+	
A	858(0)	[906]	437(0)	[458]	255(0)	[254]	173(0)	[193.5]
E	284(0)	[275]	162(0)	[178]	90(0)	[116]	58(0)	[71]
T	1134(693)	[1167]	640(496)	[662]	504(353)	[503,496]	408(80)	[410]
	412(130)	[358]	242(16)	[255]	141(3)	[148]	92(1)	[89]

symmetry	AsF_4^+		$AsCl_4^+$		$AsBr_4^+$		AsI_4^+	
A	725(0)	[748]	402(0)	[422]	242(0)	[245]	166(0)	[183]
E	192(0)	[272]	129(0)	[151]	76(0)	[83]	52(0)	[72]
T	837(223)	[825]	483(213)	[503]	353(148)	[352]	279(105)	[319]
	258(84)	[287]	173(12)	[186]	111(3)	[115]	77(1)	[87]

	frequency (cm^{-1})[b]							
symmetry	SbF_4^+		$SbCl_4^+$		$SbBr_4^+$		SbI_4^+	
A	654(0)		377(0)	[395.6]	232(0)	[234.4]	161(0)	
E	132(0)		95(0)	[121.5]	60(0)	[76.2]	42(0)	
T	720(127)		431(141)	[450.7]	306(105)	[304.9]	238(81)	
	177(96)		124(16)	[139.4]	86(6)	[92.1]	62(2)	

	frequency (cm^{-1})[b]			
symmetry	BiF_4^+	$BiCl_4^+$	$BiBr_4^+$	BiI_4^+
A	573(0)	323(0)	204(0)	142(0)
E	125(0)	86(0)	55(0)	38(0)
T	608(81)	352(21)	244(51)	183(38)
	163(69)	99(14)	70(5)	51(2)

[a] Experimental (ref 30) values are reported in square brackets. [b] Infrared intensities, in km mol^{-1}, are given in parentheses.

the latter case. In the case of the $\nu_1(A_1)$ mode, all five of the expected isotopically shifted bands were observed (Table 5) even though the spectrum of the $As(OTeF_5)_6^-$ salt suffers from overlap between the $As^{35}Cl_4^+$ band of $\nu_1(A_1)$ and an anion band at 423 cm^{-1}. The assignments of these chlorine isotopic splittings to their corresponding isotopomers are given in Table 5 and have been made by analogy with those of $SbCl_4^+$ [30] and with the isotopically split $\nu_1(A_1)$ mode of PCl_4^+.[5] The relative intensities of the isotopomer bands are in agreement with their relative natural abundances (see ref 30). The average isotopic shifts per mass unit are 1.4 cm^{-1} amu^{-1} ($\nu_1(A_1)$) and 1.9 cm^{-1} amu^{-1} ($\nu_3(T_2)$) following the anticipated mass trend; i.e., they are correspondingly smaller than in PCl_4^+ (1.5 cm^{-1} amu^{-1} for $\nu_1(A_1)$) and larger than in $SbCl_4^+$ (1.3 and 1.6 cm^{-1} amu^{-1}, respectively). The values observed for the $AsCl_4^+$ cation are equal, within experimental error (±0.1 cm^{-1}), to those obtained for the isoelectronic $GeCl_4$ molecule (1.4[66] and 1.9[67] cm^{-1} amu^{-1}, respectively). As in $SbBr_4^+$, splittings arising from the $^{79/81}Br$ isotope effect could not be resolved for $AsBr_4^+$. It is worth noting, however, that the $\nu_3(T_2)$ and $\nu_4(T_2)$ modes for $AsBr_4^+$ do reveal some splitting. A factor-group analysis (Supporting Information) shows that the splitting does not result from vibrational coupling within the unit cell of [$AsBr_4$][$AsF(OTeF_5)_5$] but from the occupation of two equally populated but inequivalent sites for the $AsBr_4^+$ cations having C_1 site symmetry. In contrast, a factor-group analysis of [$AsCl_4$][$As(OTeF_5)_6$] reveals that none of the $AsCl_4^+$ cation modes are expected to be split, thus helping to facilitate the observation of $^{35/37}Cl$ isotope splittings.

Computational Results. The results of the density functional theory calculations at the local (LDFT/DZVP) level for the PnX_4^+ cations are summarized in Table 6. Overall, there is good agreement between the calculated and observed geometrical parameters even though the calculated bond lengths tend to be longer than the experimental ones except for PBr_4^+, where they are shorter, and PI_4^+, where the two values are in excellent agreement. Consequently, the calculated vibrational frequencies are in general found to be lower than the experimental values. For the known cations, the expected bond length trends (Pn−F) < (Pn−Cl) < (Pn−Br) < (Pn−I) and (P−X) < (As−X) < (Sb−X) < (Bi−X) and the reverse trends for the frequencies are observed. On the basis of comparisons of the calculated and available experimental values, we expect the other predicted bond lengths to be too long and the frequencies to be lower than the experimental values, but still of use in assigning the spectra of new halide cations. For comparison, we also note that the calculated bond lengths for AsF_4^+ (1.666 Å) and AsI_4^+ (2.498 Å) are somewhat longer than our previous empirically estimated values of 1.606 and 2.449 Å, respectively.[30]

Conclusions

The known $AsCl_4^+$ and $AsBr_4^+$ cations have been synthesized and characterized by X-ray crystallography as their $As(OTeF_5)_6^-$ and $AsF(OTeF_5)_5^-$ salts, respectively. The $AsBr_4^+$ cation represents the second tetrahaloarsonium(V) cation to have been fully structurally characterized. Both $AsBr_4^+$ and $AsCl_4^+$ have

(66) Chumaevskii, N. A. *Russ. J. Inorg. Chem.* **1991**, *36*, 1491. Chumaevskii, N. A. *Zh. Neorg. Khim.* **1991**, *36*, 2655.
(67) Tevault, D.; Brown, J. D.; Nakamoto, K. *Appl. Spectrosc.* **1976**, *30*, 461.

been characterized for the first time in solution by ^{75}As NMR spectroscopy. While $[AsCl_4][As(OTeF_5)_6]$ is stable, $[AsBr_4][As(OTeF_5)_6]$ undergoes slow decomposition at room temperature but is kinetically more stable than the previously reported AsF_6^- salt and the presently reported $AsF(OTeF_5)_5^-$ salt, which rapidly decompose upon warming to room temperature. Analysis of the bond valence parameters associated with the long cation−anion contacts reveals that the $As(OTeF_5)_6^-$ anion is more weakly coordinating toward $AsCl_4^+$ than AsF_6^-. Density functional theory calculations have been used to calculate the geometrical parameters and vibrational frequencies of known PnX_4^+ cations and have been used to predict those of the presently unknown BiX_4^+, SbF_4^+, and SbI_4^+ cations.

Experimental Section

Materials and Apparatus. Manipulations involving volatile materials were performed under strictly anhydrous conditions as described previously.[30] *Caution*: Most of the compounds described in this work are highly toxic and must be handled on vacuum systems or in dryboxes that have pumps and ports that are correctly vented and in laboratories equipped with adequate ventilation and fume hoods. In addition, work involving the handling of glass vessels pressurized with SO_2ClF and liquid Cl_2 should be conducted with proper shielding in place.

Sulfurylchlorofluoride, SO_2ClF (Columbia Organic Chemical Co.), was purified according to the literature method.[68] Chlorine gas (Matheson) was dried by bubbling through concentrated sulfuric acid followed by condensation at −78 °C into a dry glass U-tube equipped with J. Young glass/Teflon stopcocks and stored at −78 °C until it was used. Arsenic tribromide (Strem Chemical, 99.9%) was used without further purification. Arsenic trichloride, $AsCl_3$ (BDH, >99%) and $SbCl_5$ (Eastman Kodak) were vacuum-distilled twice and stored in Pyrex glass vessels prior to use. Literature methods were used to prepare $ClOTeF_5$,[69] $B(OTeF_5)_3$,[53] $As(OTeF_5)_5$,[70] and $AgOTeF_5$.[50,71]

Preparation of $AsF(OTeF_5)_4$. It was not possible to obtain $AsF(OTeF_5)_4$ completely free of $As(OTeF_5)_5$. The preparation was similar to that used to prepare $As(OTeF_5)_5$,[70] which has been previously obtained in high purity. In a typical preparation, 1.3275 g (7.81 mmol) of AsF_5 was condensed onto 9.4889 g (13.05 mmol) of $B(OTeF_5)_3$ at −196 °C contained in one bulb of a dry double-bulb (100 mL each) glass reaction vessel equipped with a magnetic stirring bar, with a J. Young stopcock on one side and a medium porosity glass frit separating the two bulbs. The vessel and contents were allowed to warm to room temperature, whereupon the mixture liquified and BF_3 evolution took place. The mixture was allowed to stand for 24 h prior to condensing ca. 20 mL of SO_2 onto the reaction mixture, which was stirred for a further 48 h. Purification by recrystallization from liquid SO_2 was identical to that previously reported for $As(OTeF_5)_5$. The melting point of the product ranged from 25 to 30 °C. The ^{19}F NMR spectrum at −70 °C consisted of a well-resolved AB_4 spin coupling pattern (F_A, −48.6 ppm; F_B, −39.8 ppm; $^2J(^{19}F_A-^{19}F_B)$, 182 Hz; $^1J(^{125}Te-^{19}F_A)$, 3643 Hz; $^1J(^{125}Te-^{19}F_B)$, 3722 Hz) that is very similar to that of $As(OTeF_5)_5$ except that a broadened singlet (12.6 ppm; $\Delta\nu_{1/2} = 125$ Hz) corresponding to fluorine directly bonded to arsenic also appears. The relative integrated intensities of the F-on-Te region (inclusive of ^{125}Te and ^{123}Te satellites) to the F-on-As region was 20:1. The singlet was presumably broadened by the unresolved four-bond scalar couplings to the axial and equatorial fluorines on tellurium and/or by the nearly quadrupole collapsed $^1J(^{75}As-^{19}F)$ coupling. The observation of a single AB_4 pattern at low temperature is consistent with a trigonal pyramidal arrangement of F and $OTeF_5$ ligands undergoing rapid intramolecular exchange by means of a Berry-style pseudorotation mechanism.

Preparation of High-Purity $BrOTeF_5$. The synthesis of $BrOTeF_5$ is an improved version of the published method.[72] In a typical synthesis, $ClOTeF_5$ (1.7750 g, 9.104 mmol; 5.3 mol % excess) was condensed at −196 °C into a preweighed 100 mL Pyrex glass bulb equipped with a J. Young stopcock, followed by condensation of Br_2 (0.6905 g, 4.321 mmol) into the bulb at −196 °C. The mixture was allowed to react at room temperature in the dark for 12 h, forming an orange-brown vapor over a dark-red liquid. The reaction vessel was connected to a series of two dry glass U-traps, and the vessel was cooled to −20 °C. The contents were slowly pumped through traps cooled to −45 and −78 °C, respectively, to remove excess $ClOTeF_5$. A ruby-red liquid was collected at −45 °C, whereas an orange solid was collected at −78 °C. The −45 °C trap was warmed to room temperature, and all the material was distilled into the −78 °C trap. The cold baths were then exchanged and the product pumped in the opposite direction over a period of 90 min, collecting the product in the −45 °C trap. The final product was a deep-ruby-red liquid; yield 2.7375 g (8.595 mmol, 99.5% based on the total amount of Br_2), mp −52 °C (reported value −75 °C).[72] The ^{19}F NMR spectrum of the product in SO_2ClF solvent at −50.3 °C showed a single AB_4 pattern (F_A, −47.2 ppm; F_B, −53.9 ppm; $^2J(^{19}F_A-^{19}F_B)$, 180 Hz; $^1J(^{125}Te-^{19}F_A)$, 3419 Hz; $^1J(^{125}Te-^{19}F_B)$, 3788 Hz) and no detectable impurities.

Syntheses of $[AsCl_4][As(OTeF_5)_6]$, $[AsBr_4][As(OTeF_5)_6]$, $[AsBr_4][AsF(OTeF_5)_5]$, and $[AsCl_4][Sb(OTeF_5)_{6-n}Cl_n]$. (a) $[AsCl_4][As(OTeF_5)_6]$. In the drybox $As(OTeF_5)_5$ (1.0573 g, 0.8339 mmol) was loaded into a 7 mm glass tube equipped with a 4 mm J. Young stopcock. On the vacuum line, 0.1576 g (0.8693 mmol) of $AsCl_3$ and 0.2909 g (1.0615 mmol) of $ClOTeF_5$ were distilled into the tube at −196 °C and the mixture was allowed to warm to and remain at room temperature overnight. Excess $ClOTeF_5$ was removed by pumping first at −78 °C and then at room temperature to give a white powder. The product was returned to the drybox and loaded into a two-arm glass crystallization vessel where it was recrystallized from SO_2ClF. To obtain crystals suitable for X-ray crystallography, the solution was cooled from 45 °C to room temperature over several days in a water bath. Transparent, well-defined, hexagonal crystals appeared and were isolated by sealing off one arm of the reactor.

(b) $[AsBr_4][As(OTeF_5)_6]$ and $[AsBr_4][AsF(OTeF_5)_5]$. In the drybox, $AsF(OTeF_5)_4$ containing ca. 5−10 mol % $As(OTeF_5)_5$ (0.8021 g) was transferred in a two arm $^1/_4$ in. o.d. FEP tube. The tube was cooled to below −100 °C, and $AsBr_3$ (0.2016 g, 0.6407 mmol) was added. The cold tube was removed from the drybox and maintained at −78 °C until SO_2ClF (ca. 3 mL) was distilled into the tube. The $BrOTeF_5$ was distilled into a preweighed graduated glass tube, and 0.2111 g (0.6628 mmol) was distilled from there into the reaction tube. The sample was warmed briefly to 0 °C and mixed, and about 0.5 mL of SO_2ClF was rapidly pumped off. Crystals were grown at −30 °C, slowly decreasing the temperature to −38 °C over a period of 8 h. During this period large well-formed tablet-shaped crystals were deposited on the walls. The sample was cooled to −45 °C, and the solvent was decanted into the sidearm. The sidearm was then cooled with liquid N_2 and heat-sealed off under vacuum. Samples for Raman and ^{19}F NMR spectroscopic studies were prepared in a similar manner by mixing the reagents at −78 °C in SO_2ClF and rapidly pumping to dryness at 0 °C. The resulting pale-yellow powder was transferred at low temperature (ca. −100 to −120 °C) inside a drybox into the appropriate glass sample tubes, which were closed and removed from the drybox. In the case of the NMR samples, SO_2ClF solvent was condensed into the sample tubes at −196 °C and all tubes were heat-sealed at −196 °C. Samples for ^{75}As NMR spectroscopy were prepared directly from the reagents $BrOTeF_5$ and $AsF(OTeF_5)_4$, as described above, in 10 mm thin-wall glass NMR tubes and heat-sealed with SO_2ClF solvent. All samples were stored at −78 °C or lower until their spectra or crystal structure could be determined.

(c) $[AsCl_4][Sb(OTeF_5)_{6-n}Cl_n]$. The procedure for the preparation of $AgSb(OTeF_5)_6$ was similar to that reported previously except that the reaction was carried out in SO_2ClF solvent. The reagents $SbCl_5$ (0.5098 g, 1.705 mmol) and $AgOTeF_5$ (5.5612 g, 10.28 mmol) were transferred into the central arm and into one of the sidearms of a three-arm glass reaction vessel, which was equipped with three 4 mm J. Young stopcocks and two medium porosity glass frits separating the

(68) Schrobilgen, G. J.; Holloway, J. H.; Granger, P.; Brevard, C. *Inorg. Chem.* **1978**, *17*, 980.
(69) Seppelt, K.; Turowsky, L. *Z. Anorg. Allg. Chem.* **1990**, *590*, 37.
(70) Collins, M. J.; Schrobilgen, G. J. *Inorg. Chem.* **1985**, *24*, 2608.
(71) Strauss, S. H.; Noirot, M. O.; Anderson, O. P. *Inorg. Chem.* **1985**, *24*, 4307.
(72) Seppelt, K. *Chem. Ber.* **1973**, *106*, 1920.

central arm from the two sidearms. After 15 mL of SO_2ClF was distilled onto the $SbCl_5$, the resulting clear solution was poured through one frit onto the $AgOTeF_5$, yielding a pale-yellow precipitate of AgCl and a pale-yellow solution. After the reaction mixture was agitated in the dark over a period of 3 days, the solution above the precipitate was filtered through one frit into the central arm. The volume of the filtrate was reduced, resulting in further precipitation. After repeated extraction of the reaction mixture, the solution in the central arm was filtered into the third arm of the reaction vessel. The SO_2ClF solvent was removed under dynamic vacuum, yielding a white solid that was studied by ^{19}F NMR spectroscopy and Raman spectroscopy. The ^{19}F NMR spectrum of the product (eq 16) redissolved in SO_2ClF revealed that it contained several weak, severely overlapping AB_4 patterns in the range -39 to -52 ppm with a strong central feature at -42.7 ppm corresponding to $Sb(OTeF_5)_6^-$ (-42.5 ppm in the $N(CH_3)_4^+$ salt in CH_3CN solvent at 30 °C). The additional AB_4 patterns are attributed to the mixed anion series $Sb(OTeF_5)_{6-n}Cl_n^-$. Weak Raman bands assigned to Sb−Cl stretchs were observed at 329 and 337 cm^{-1} in the solid.

In a drybox, 1.057 g $[Ag][Sb(OTeF_5)_{6-n}Cl_n]$ was loaded into one arm of a dry two-arm glass reaction vessel equipped with a medium porosity glass frit. Arsenic trichloride (0.1208 g, 0.666 mmol) was condensed into the opposite arm from a preweighed vessel, and ca. 10 mL of SO_2ClF was condensed onto the $AsCl_3$ and warmed to room temperature. The solution was poured through the frit onto the $[Ag][Sb(OTeF_5)_{6-n}Cl_n]$, whereupon a precipitate of AgCl formed. The mixture was agitated in the dark for 24 h and filtered back through the glass frit. The precipitate was washed several times with aliquots of back-distilled SO_2ClF. Removal of the solvent under vacuum yielded 0.6813 g of a white powder. After removal of a sample for Raman spectroscopy, the remaining sample (0.6263 g) was transferred to a dry 10 mm glass tube glass-blown onto a length of $^1/_4$ in. o.d. glass tubing and attached to a 4 mm J. Young stopcock by means of a $^1/_4$ in. stainless steel Cajon Ultra-Torr union and 1.1238 g (15.85 mmol) of Cl_2 was condensed onto the sample. Upon heat-sealing the $^1/_4$ in. o.d. portion of the sample tube under dynamic vacuum at -196 °C, the reaction tube was slowly warmed to and allowed to stand at room temperature for 5 days under a layer of liquid Cl_2. The reaction vessel was cut open on the $^1/_4$ in. portion of the reactor inside a drybox at -100 to -120 °C, a dry J. Young stopcock was reattached through a Cajon Ultra-Torr union, and the cold sample was removed from the drybox. The Cl_2 was removed by pumping the sample first at -78 °C and then at room temperature, yielding a white powder.

Crystal Structure Determinations of $[AsCl_4][As(OTeF_5)_6]$ (-123 and -183 °C) and $[AsBr_4][AsF(OTeF_5)_5]$ (-183 °C). Collection and Reduction of X-ray Data. Crystals of both salts were stored at -78 °C prior to mounting on the diffractometer. The data were collected on a Stoe imaging plate diffractometer system equipped with a one-circle goniometer and a graphite monochromator. Monochromatic Mo Kα radiation at $\lambda = 0.710\,73$ Å was used. The temperature was regulated within ±1 °C using an adjustable cold N_2 flow. In all cases, corrections for Lorentz and polarization effects were carried out and no absorption correction was applied.

(a) $[AsCl_4][As(OTeF_5)_6]$. Crystal data were collected on a single crystal with dimensions 0.49 mm × 0.40 mm × 0.23 mm. Some reflections could not be indexed because of the presence of small fragments attached to the main crystal. A preliminary lattice constant determination at 0 °C yielded a rhombohedral unit cell with $a = 9.8741(14)$ Å and $c = 55.301(11)$ Å. The crystal was slowly cooled to -123 °C at a rate of 8 °C/h. Data were collected at this temperature, and the orientation matrix and lattice parameters were redetermined. Twenty exposures of 4 min with a separation of $\Delta\phi = 18°$ were obtained, which showed 1994 reflections from which 1622 matched the predetermined unit cell. To obtain more intensity, data were collected in two stages: 433 exposures of 4 min were obtained at 55 mm with $10.5° \le 2\theta \le 56°$ and with the crystal oscillated through 0.3° in $\Delta\phi$, and 140 exposures of 2 min were obtained at 125 mm with $10.5° \le 2\theta \le 56°$ and with the crystal oscillated through 1° in $\Delta\phi$. The two data sets were merged to yield a total of 10 828 reflections, which could be reduced to 2516 unique reflections.

For a second data set the temperature was lowered to -183 °C at a rate of 5 °C/h. Indexing yielded a doubling of the a axis ($a = 19.6881(14)$ Å and $c = 55.264(11)$ Å). The reflections became broader and were split at higher angles. A total of 47 032 reflections could be reduced to 11 012 unique reflections.

The temperature for the phase transition was determined by warming the crystal slowly and determining the orientation matrix. A reversible phase transition takes place at -155 °C.

(b) $[AsBr_4][AsF(OTeF_5)_5]$. Crystal data were collected on a single crystal with dimensions 0.17 mm × 0.15 mm × 0.11 mm. A lattice constant determination at -183 °C yielded a triclinic unit cell with $a = 9.778(4)$ Å, $b = 17.731(7)$ Å, $c = 18.870(8)$ Å, $\alpha = 103.53(4)°$, $\beta = 103.53(4)°$, and $\gamma = 105.10(4)°$. Data were collected in two stages: 440 exposures of 3 min were obtained at 75 mm with $30° \le 2\theta \le 140°$ and with the crystal oscillated through 0.5° in $\Delta\phi$, and 183 exposures of 2 min were obtained at 125 mm with $30° \le 2\theta \le 140°$ and with the crystal oscillated through 1.2° in $\Delta\phi$. The two data sets were merged to yield a total of 10 508 reflections, which could be reduced to 7008 unique reflections. It should be noted that 20 crystals from two different samples were examined, and they all gave rise to the same unit cell; i.e., no evidence for the $[AsBr_4][As(OTeF_5)_6]$ salt could be found.

Solution and Refinement of the Structures. All calculations were performed on a Silicon Graphics, Inc., model 4600PC workstation using the SHELXTL-*Plus* package (Sheldrick, 1994)[73] for structure determination, refinement, and molecular graphics. The numerical values for the -183 °C data set ($AsCl_4^+$), when they differ from those of the -123 °C data set ($AsCl_4^+$), are given in parentheses; those for $AsBr_4^+$ at -183 °C are given in square brackets.

The XPREP program[73] was used to confirm the unit cell dimensions and the crystal lattices. The solutions were obtained by using conventional direct methods that located the general and/or special positions of all heavy atoms. Successive difference Fourier syntheses revealed the remaining positions of all chlorine, bromine, fluorine, and oxygen atoms. Any disorder in the anions was modeled at this point in the refinement, while crystallographically well-behaved cations and anions were refined with anisotropic thermal parameters. The positions of the oxygen atoms for the "As(3)" ("As(5)" and "As(6)") of the $As(OTeF_5)_6^-$ anions could be separated. The disorder could be described as an orientational disorder involving four (two) anions sharing the same central arsenic atom and the same tellurium atoms in which the oxygen atoms were separated by about 0.87 (0.79, 0.93) Å. The positions of the F atoms could not be split, even though their large thermal parameters indicated that they were also suffering from the same positional disorder. The structure was solved using a disorder model where the As−O and O−Te distances were restrained to those in the ordered $As(OTeF_5)_6^-$ anions, and the site occupancy factor was adjusted accordingly. During the final stages of the refinement, all reflections with $F^2 < -2\sigma(F^2)$ were suppressed and weighting factors recommended by the refinement program were introduced. The final refinement gave rise to a residual, R_1, of 0.0438 ($wR_2 = 0.1445$) (0.1341 (0.4246)) [0.0368 (0.0513)]. In the final difference map, the maximum and the minimum electron densities were 1.223 (10.901) [2.533] and -1.867 (-3.980) [-2.120] e $Å^{-3}$. The high residual for the data set of $AsCl_4^+$ at -183 °C is due to the very large number of very weak reflections at high angles.

Nuclear Magnetic Resonance Spectroscopy. Nuclear magnetic resonance spectra were recorded unlocked (field drift of <0.1 Hz h^{-1}) on a Bruker AC-300 (7.0463 T) spectrometer equipped with an Aspect 3000 computer. Variable temperature spectra were obtained using a Eurotherm B-VT-2000, and probe temperatures were determined by inserting a copper constantan thermocouple directly into the probe. The ^{19}F NMR spectra were obtained using a 5 mm $^1H/^{13}C/^{19}F/^{31}P$ combination probe. Spectra were recorded in 5 mm thin-wall precision glass tubes. The $^{121,123}Sb$ and ^{75}As NMR spectra were obtained by using a broad-band probe tunable over the frequency range 14−122 MHz. Spectra were recorded in 9 mm FEP tubes. The FEP tubes were placed inside a 10 mm o.d. Wilmad precision thin-wall glass NMR tube before being placed in the probe. The FEP tubes were heat-sealed under dynamic vacuum using a small diameter Nichrome wire resistance

(73) Sheldrick, G. M. *SHELXTL-Plus*, release 5.03; Siemens Analytical X-ray Instruments, Inc.: Madison, WI, 1994.

furnace. The respective nuclei were referenced as previously described.[48] The ^{19}F NMR spectra were recorded at 282.409 MHz and accumulated in 32K (64K) memories using spectral width settings of 25 (100) kHz, acquisition times of 0.655 (0.328) s, and a data point resolution of 1.53 (3.05) Hz/data point (2000−8000 scans). The ^{121}Sb spectra at 71.83 MHz were recorded in 32K memories using spectral width settings of 100 kHz, acquisition times of 0.164 s, and a data point resolution of 6.10 Hz/data point (4000 scans). The ^{75}As NMR spectra were recorded at 51.391 MHz in 32K memories using spectral width settings of 100−50 kHz, acquisition times of 0.164−0.328 s, and data point resolutions of 3.05−6.10 Hz/data point (3000−12000 scans).

Spin−lattice relaxation measurements were performed using a regular inversion−recovery experiment (pulse sequence: $\pi-\tau-\pi/2-$acquisition) at room temperature on a Bruker AC-300 NMR spectrometer. A pulse width of 11.5 μs was used for the 90° pulse of ^{75}As. The number of transients accumulated for the determination of the ^{75}As T_1 values of the cation and the anion in $[AsCl_4][As(OTeF_5)_6]$ ($[AsBr_4][As(OTeF_5)_6]$) were 1000 and 1000 (100 and 500), respectively, and were acquired with spectral width settings of 25 (15) kHz in 16K (16K) memory. The free induction decays were processed with line broadenings of 30 (20) Hz and 30 (30) Hz for the cation and the anion, respectively. The number of τ values was 15 (10) and 15 (12) including $\tau_4 = 0.01$ and 0.01 s ($\tau_\infty = 0.5$ and 0.01 s) for the cation and the anion, respectively. Because of slow decomposition of $[AsBr_4][As(OTeF_5)_6]$, spectra were recorded with $\tau_\infty = 0.01$ s at the beginning, in the middle, and at the end of the data acquisition. The integrals were corrected assuming a linear decomposition of $[AsBr_4][As(OTeF_5)_6]$ with time. The T_1 values were obtained as the negative inverse slope of the linear plot $\ln(I_\infty - I_\tau)$ versus τ using corrected integrals. For the salt, $[AsCl_4][As(OTeF_5)_6]$, T_1 values were obtained by iterative exponential fitting of the intensity values versus τ using standard Bruker software and from the linear plot of $\ln(I_\infty - I_\tau)$ versus τ.

Raman Spectroscopy. The Raman spectra of $[AsCl_4][As(OTeF_5)_6]$ (−124 °C, macrochamber), $[Ag/AsCl_4][Sb(OTeF_5)_{6-n}Cl_n]$, and $[Ag/AsCl_4][Sb(OTeF_5)_{6-n}Cl_{n-2}/Sb(OTeF_5)_{6-n}Cl_n]$ (24 °C, microchamber) were recorded on a Jobin-Yvon Mole S-3000 triple spectrograph system as previously described.[30] The 514.5 nm line of a Spectra Physics model 2016 Ar^+ ion laser was used for excitation of the samples.

The Raman spectrum of $[AsBr_4][AsF(OTeF_5)_5]$ was recorded on a Bruker RFS 100/S FT Raman spectrometer equipped with a R495 low-temperature accessory and employed a quartz beam splitter and a liquid nitrogen cooled Ge diode detector. The backscattered (180 °C) radiation was sampled, and spectra were corrected for instrument response. The scanner velocity was 5 kHz, and the wavelength range for acquisition was 5894−10394 cm^{-1} when shifted relative to the laser line at 9395 cm^{-1}, giving a spectral range of 3501 to −999 cm^{-1}. The Fourier transformations were carried out by using a Blackman Harris four-term apodization and a zero-filling factor of 2. The 1064 nm line of a Nd:YAG laser (400 mW maximum output) was used for excitation of the samples with a laser spot diameter below 0.1 mm. The spectrum was recorded at −110 °C with a resolution of 1 cm^{-1}, a laser power of 150 mW, and 400 scans, and a white-light correction was subsequently applied.

Calculations. All calculations were done with the density functional theory program DGauss[74−76] on SGI computer systems. For the calculations on PF_4^+ and PCl_4^+, the DZVP2 basis set[77] for P and F was used with the A1 fitting set. For PBr_4^+ and PI_4^+, the DZVP basis set was used with the A1 fitting set. For all of the halides with M = As and Sb, the DZVP basis set with the A1 fitting set was used. The calculations on the bismuth halides were done with the Hay−Wadt ECP and basis set[78] on Bi with the pseudopotential fitting sets in Unichem.[79] For F and Cl, the DZVP2 basis set was used with the A1 fitting set, and for Br and I, the DZVP basis set was used with the A1 fitting sets. All calculations were done at the local level with the potential fit of Vosko, Wilk, and Nusair.[80] The geometries were optimized by using analytic gradient methods, and second derivatives were also calculated analytically.[81]

Acknowledgment. We thank the donors of the Petroleum Research Fund, administered by the American Chemical Society, for support of this work under Grant ACS−PRF No. 26192-AC3 (G.J.S.), the Natural Sciences and Engineering Research Council of Canada for a research grant (G.J.S.), the Ontario Ministry of Education and Training for the award of a graduate scholarship (M.G.). This research was performed in part using the Molecular Science Computing Facility (MSCF) in the William R. Wiley Environmental Molecular Sciences Laboratory at the Pacific Northwest National Laboratory. The MSCF is funded by the Office of Biological and Environmental Research in the U.S. Department of Energy. Pacific Northwest is operated by Battelle for the U.S. Department of Energy under Contract DE-AC06-76RLO 1830. We gratefully acknowledge Prof. A. Simon, Max-Planck-Institut, Stuttgart, for making the Stoe imaging plate diffractometer system available. We thank Markus Brandhorst for his assistance with the preparation of $AsF(OTeF_5)_4$.

Supporting Information Available: Arsenic-75 T_1 measurements of $[AsBr_4][As(OTeF_5)_6]$ and $[AsCl_4][As(OTeF_5)_6]$ at 30 °C in SO_2ClF solvent, factor-group analyses for $[AsCl_4][As(OTeF_5)_6]$ and $[AsBr_4][AsF(OTeF_5)_5]$, and an X-ray crystallographic file in CIF format for the structure determinations of $[AsCl_4][As(OTeF_5)_6]$ and $[AsBr_4][AsF(OTeF_5)_5]$. This material is available free of charge via the Internet at http://pubs.acs.org.

IC000118G

(74) Andzelm, J.; Wimmer, E.; Salahub, D. R. In *The Challenge of d and f Electrons: Theory and Computation*; Salahub, D. R., Zerner, M. C., Eds.; ACS Symposium Series 394; American Chemical Society: Washington DC, 1989; p 228.
(75) Andzelm, J. In *Density Functional Theory in Chemistry*; Labanowski, J., Andzelm, J., Eds.; Springer-Verlag: New York, 1991; p 155.
(76) Andzelm, J.; Wimmer, E. *J. Chem. Phys.* **1992**, *96*, 1280. DGauss is a density functional program that is part of Unichem and is available from Oxford Molecular. Versions 4.1 and 5.0 Beta were used.
(77) Godbout, N.; Salahub, D. R.; Andzelm, J.; Wimmer, E. *Can. J. Chem.* **1992**, *70*, 560.
(78) Hay, P. J.; Wadt, W. R. *J. Chem. Phys.* **1985**, *82*, 271, 285, 299.
(79) Lee, C.; Chen, H. Unpublished results. See the Unichem manual, version 3.0.
(80) Vosko, S. J.; Wilk, L.; Nusair, W. *Can. J. Phys.* **1980**, *58*, 1200.
(81) Komornicki, A.; Fitzgerald, G. *J. Phys. Chem.* **1993**, *98*, 1398 and references therein.